Modeling of the ring current with IMPTAM

Natalia Ganushkina

(1)   Finnish Meteorological Institute, Helsinki, Finland
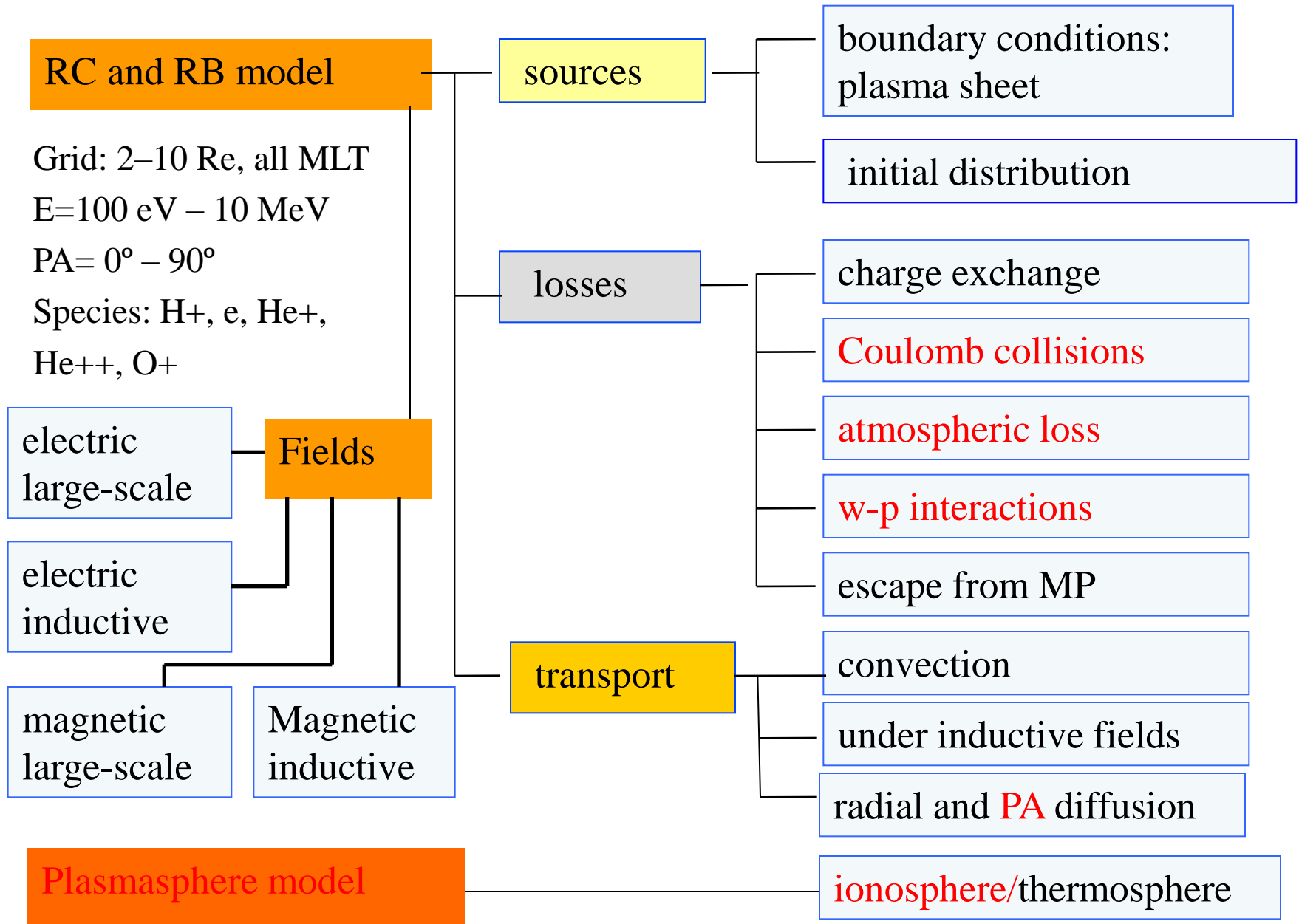*(2)   University of Michigan, Ann Arbor MI, USA*

First meeting of ISSI Team "Ring current modeling: Uncommon Assumptions and Common Misconceptions", March 7-11, 2016, Bern, Switzerland

IMPTAM

Inner Magnetosphere Particle Transport and Acceleration Model

Inner Magnetosphere Particle Transport and Acceleration Model

RC and RB model

Grid: 2–10 Re, all MLT

E=100 eV – 10 MeV

PA= 0º – 90º

Species: H+, e, He+,

He++, O+

electric large-scale

electric inductive

Fields

magnetic large-scale

Magnetic inductive

Plasmasphere model

sources

- boundary conditions: plasma sheet
- initial distribution

losses

- charge exchange
- Coulomb collisions
- atmospheric loss
- w-p interactions
- escape from MP

transport

- convection
- under inductive fields
- radial and PA diffusion

ionosphere/thermosphere

Inner Magnetosphere Particle Transport and Acceleration Model (IMPTAM)

The inner magnetosphere particle transport and acceleration model:
- follows distributions of ions and electrons with arbitrary pitch angles
- from the plasma sheet to the inner L-shell regions
- with energies reaching up to hundreds of keVs
- in time-dependent magnetic and electric fields.
- distribution of particles is traced in the guiding center, or drift, approximation
    (motion of a charged particle as displacements of its guiding center,
    or the center of the circular Larmor orbit of a moving particle).

References:
1. Ganushkina, N. Yu., Pulkkinen, T. I., Fritz, T., Role of substorm-associated impulsive electric fields in the ring current development during storms, Ann. Geophys., 23, 579-591, 2005.
2. Ganushkina, N., Pulkkinen, T. I., Liemohn, M. and Milillo, A., Evolution of the proton ring current energy 670 distribution during April 21-25, 2001 storm, J. Geophys. Res., 111, A11S08, doi:10.1029/2006JA011609, 2006
3. Ganushkina, N. Yu., M. W. Liemohn, and T. I. Pulkkinen, Storm-time ring current: Model-dependent results, Annales Geophysicae, 30, 177-202, 2012.

Inner Magnetosphere Particle Transport and Acceleration Model (1)

In order to follow the evolution of the particle **distribution function** f and particle **fluxes** in the inner magnetosphere dependent on the **position, time, energy, and pitch angl**e , it is necessary to specify:

(1) particle distribution at initial time at the model boundary;
(2) magnetic and electric fields everywhere dependent on time;
(3) drift velocities;
(3) all sources and losses of particles.

Inner Magnetosphere Particle Transport and Acceleration Model (5)

Losses for ions:
- **charge exchange** with Hydrogen from geocorona;
- **Coulomb interaction** in dense thermal plasmas (plasmasphere);
- **convection outflow**, particle intersects the magnetopause and flows away along magnetosheath magnetic field lines.

Losses for electrons:
- **Coulomb collisions** and loss to the atmosphere;
- **convection outflow**, particle intersects the magnetopause and flows away along magnetosheath magnetic field lines;
- scattering into the loss cone due to **pitch angle diffusion**.

Ring current studies, ions

Q1: What are the common/uncommon assumptions we make and should they be revisited?

Electric and Magnetic Fields
Initial and Boundary Conditions

Combinations of models for IMPTAM for July 21-23, 1997 storm

No self-consistency (special subject for separate study)

	Electric Field	Boundary conditions
dipole	Volland-Stern	Tsyganenko and Mukai, 2003
T89	Volland-Stern	Tsyganenko and Mukai, 2003
T96	Volland-Stern	Tsyganenko and Mukai, 2003
TS04	Volland-Stern	Tsyganenko and Mukai, 2003
dipole	Boyle et al., 1997	Tsyganenko and Mukai, 2003
T89	Boyle et al., 1997	Tsyganenko and Mukai, 2003
T96	Boyle et al., 1997	Tsyganenko and Mukai, 2003
TS04	Boyle et al., 1997	Tsyganenko and Mukai, 2003

Best fit with observed Dst for **dipole** + **T96** + **VS** model combination

Model-dependent Dst calculations during storms

1. Using **Dessler-Parker-Sckopke relationship**:

The energy in the ring current can be expressed by $\boxed{\dfrac{\Delta\vec{B}}{B_E} = -\dfrac{2}{3}\dfrac{W_{RC}}{W_{mag}}\hat{k}}$, where

$W_{mag} = \dfrac{4\pi}{3\mu_0}B_E^2 R_E^3$ is the total energy in the Earth's dipole magnetic field above the surface, B_E is the magnetic field at the Earth's surface, R_E is one Earth radii (6371 km).

$\Delta\vec{B}$ is the change in B measured at the surface of the Earth (Dst).

2. Calculating from the model ring current by **Biot-Savart law**:

The magnetic disturbance parallel to the earth's dipole at the center of the earth ΔB induced by the azimuthal component of $J_\perp$, is given by

$$\boxed{\Delta B = \dfrac{\mu_0}{4\pi}\int_r \int_\lambda \int_\phi \cos^2\lambda J_\phi(r,\lambda,\phi)\,dr\,d\lambda\,d\phi}$$

$$\vec{j}_\perp = \dfrac{\vec{B}}{B^2}\times\left(\nabla P_\perp + \dfrac{P_{II}-P_\perp}{B^2}(\vec{B}\cdot\nabla)\vec{B}\right)$$

Dst: November 6-7, 1997 storm, boundary at 6.6 Re

kappa at 6.6 Re, n, $T_{||}$ and $T_{\perp}$ from LANL

Dipole
T89
T96
TS04
Dst_obs

(a) Biot-Savart, VS
(b) DPS, VS
(c) Biot-Savart, Boyle
(d) DPS, Boyle

Nov 6, 97   Nov 7, 97   UT
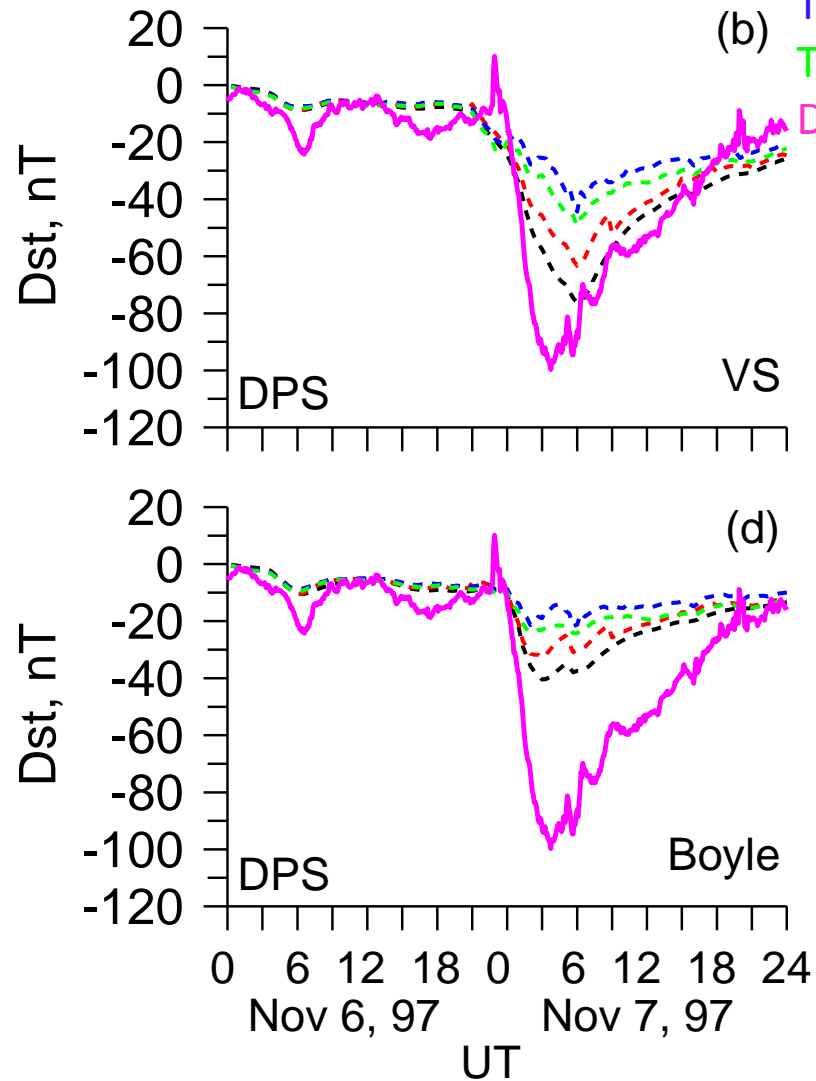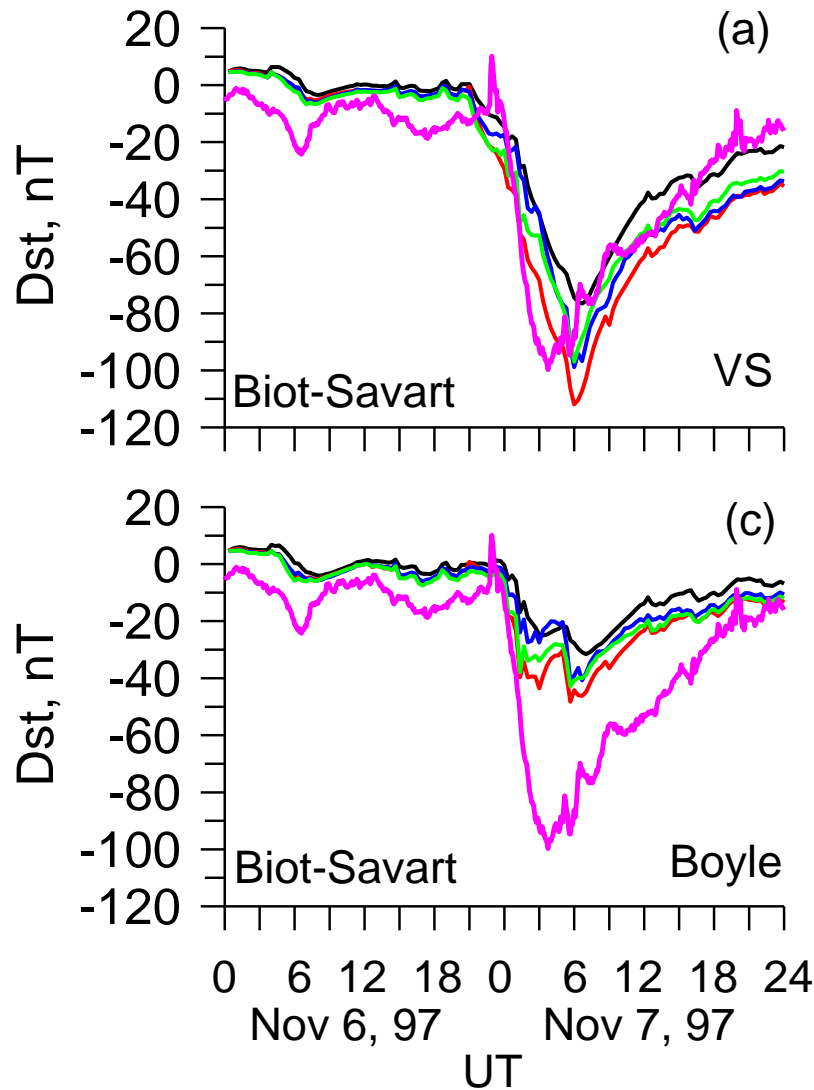
Dst: November 6-7, 1997 storm, boundary at 10 Re

Kappa at 10 Re, T and n from Tsyganenko and Mukai (2003)

Dipole
T89
T96
TS04
Dst_obs
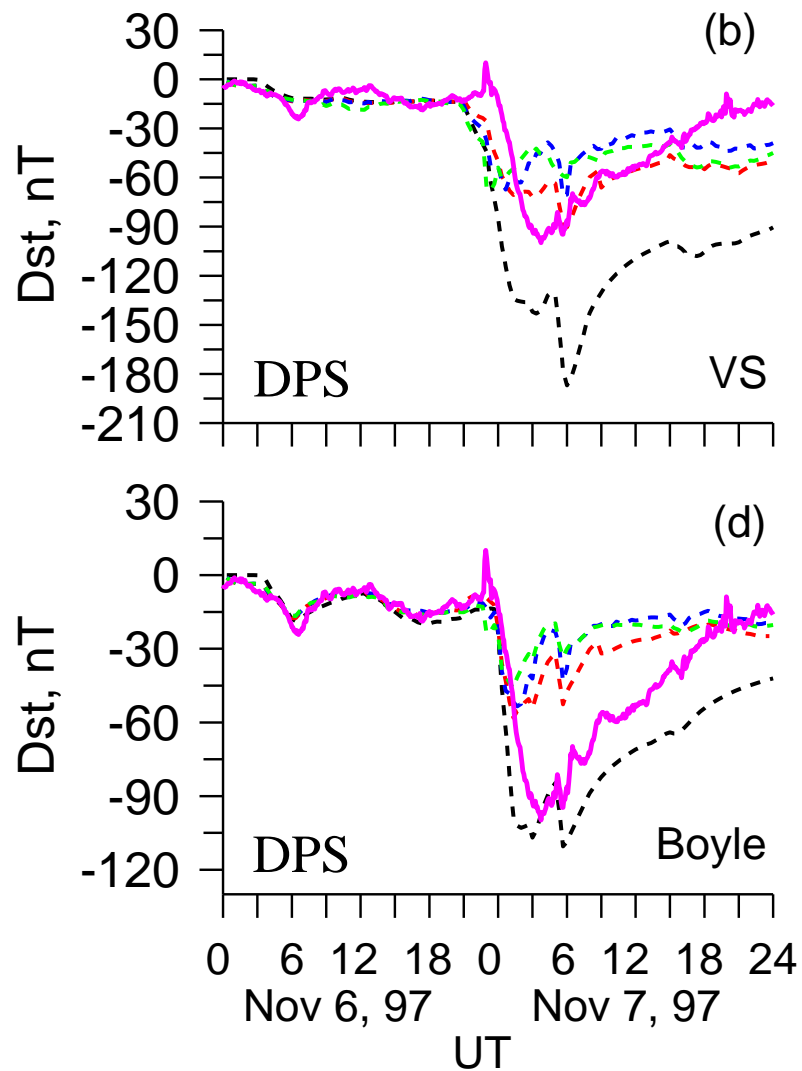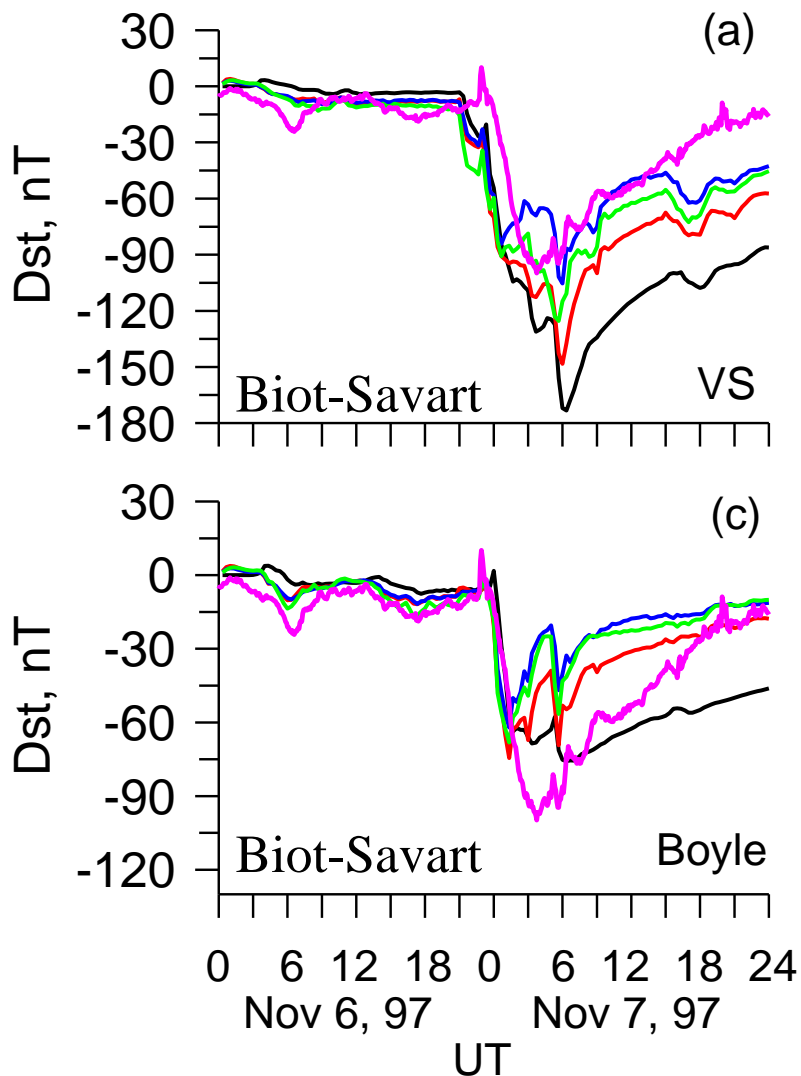
Summary (1)

- Choice of magnetic field model: For all cases simple models like dipole and T89(Kp) give the best energy density and Dst
- Choice of electric field model: polar cap potential model by Boyle et al. (SW, IMF) produces 2 times smaller values than VS(Kp) in the equatorial plane
- Choice of boundary conditions: Change from constant to variable distribution at 6.6 Re resulted in 5 times increase in energy density and Dst

Different combinations of the magnetic and electric field models and boundary conditions result in very different modeled ring current, and, therefore, the physical conclusions based on simulation results can differ significantly.

- Change the boundary position from 6.6 Re to 10 Re: resulted in further increase by 2 times of energy density and overestimation of Dst by about 100 nT

A time-dependent model boundary outside of 6.6 RE gives a possibility to take into account the particles in the transition region (between dipole and stretched field lines) forming a partial ring current and near-Earth tail current in that region.

- Method of Dst calculation: DPS and Bio-Savart approach give close values for dipole magnetic field but can differ of about 50 -100 nT for realistic magnetic field

Calculating the model Dst* by Biot-Savart's law instead of the widely used Dessler-Parker-Sckopke (DPS) relation gives larger and more realistic values, since the contribution of the near-Earth tail current can be present.

Tail current is important and has to be considered.

Q1: What are the common/uncommon assumptions we make and should they be revisited?

Electric and Magnetic Fields - Substorms

Contributions to RC energy from protons with different energy ranges: 27 storms' statistics from Polar CAMMICE/MICS data
(*Ganushkina et al., 2005*)
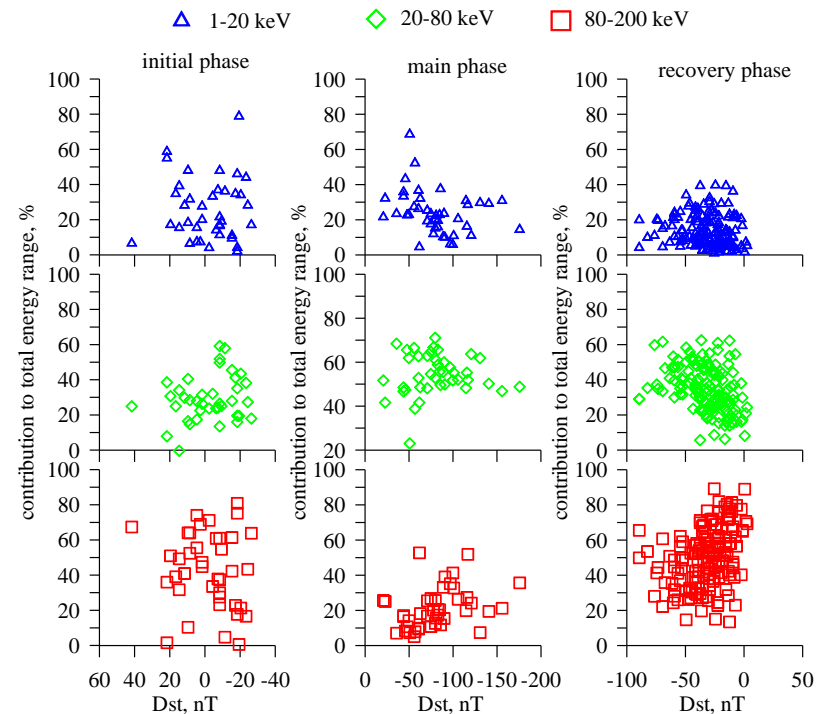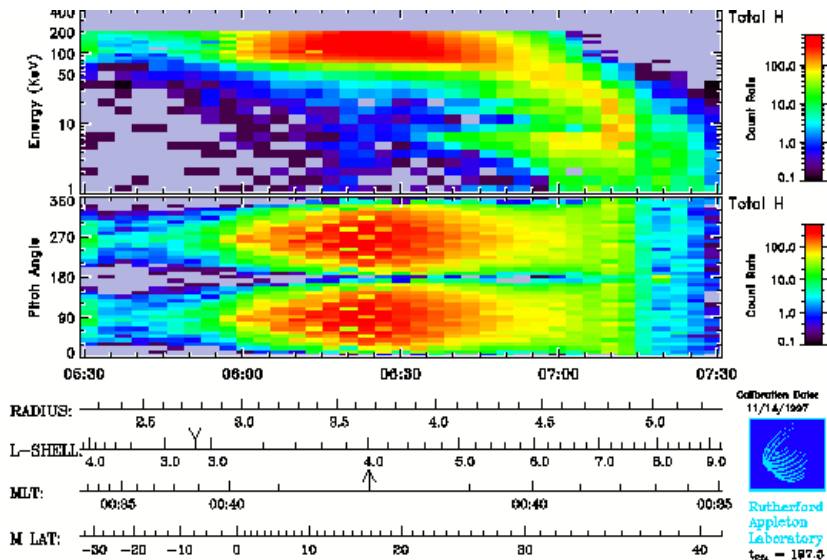
Polar orbit, years 1996-1998

- 1.8 x 9 Re, 86º incl.,
- 18 h period,
- ions of 1-200 keV

Storm main phase: **medium** energies (20-80 keV)
Storm recovery phase: **high** energies (80-200 keV)

October 21-23, 2001 storm: Energy density
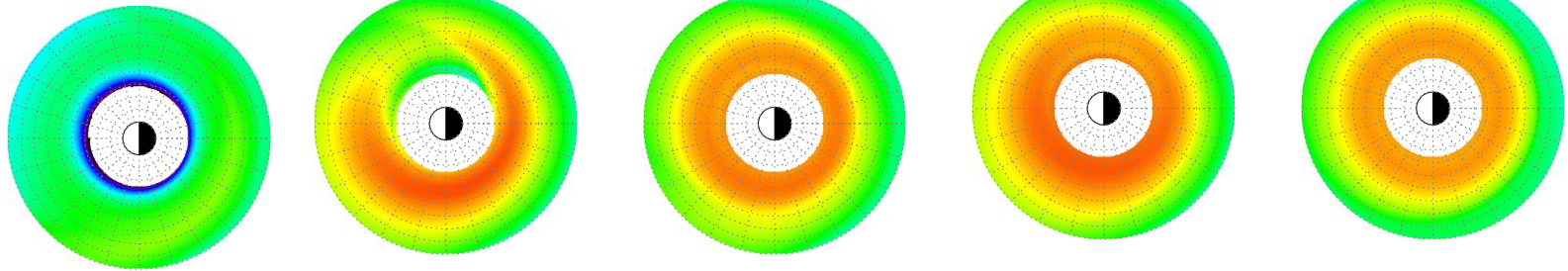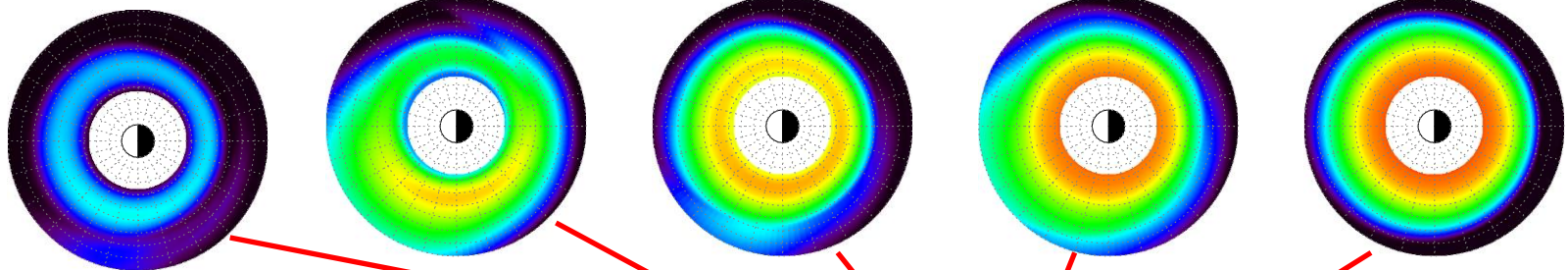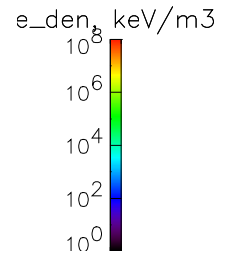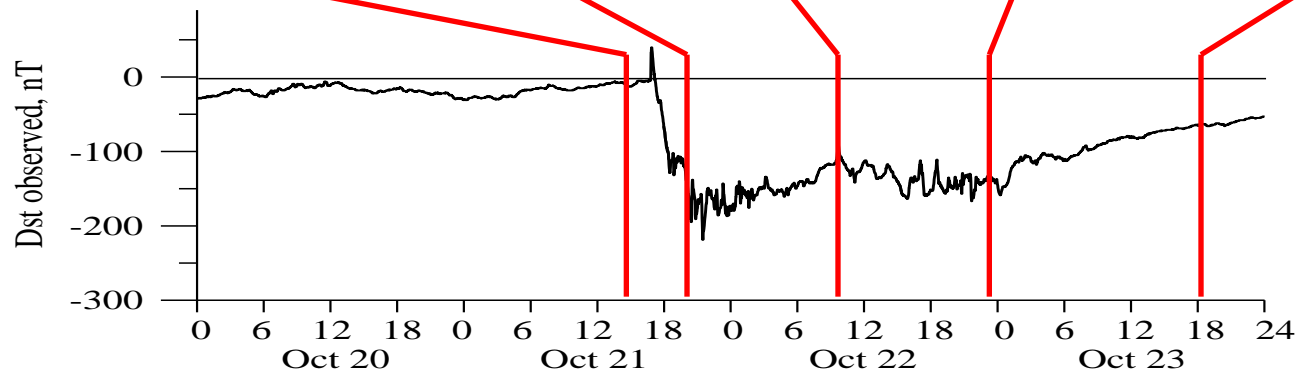
Impulsive electric fields in the Earth's inner magnetosphere: Observations and models

- Energetic particle **injections** are important manifestations of substorm expansion phase (*Arnoldy and Chan, 1969; Belian et al., 1978, 1984; Reeves et al., 1991*).

- **Electric field behaviour** is important to understand how particle injections are formed.

- **Intense (a few mV/m) electric fields** with a strong pulsed component have been detected deep in the inner magnetosphere during substorms (*Sheperd et al., 1980; Aggson et al., 1983; Maynard et al., 1983, 1996; Rowland and Wygant, 1998; Tu et al., 2000*).

- **Injection front model** (*Moore et al., 1981*): Particles are transported towards the Earth by a compressional wave front that propagates earthward from a disturbance occurring in the magnetotail.
  Russell and McPherron, 1973: propagation speed 150 km/s between 9 and 6.6 Re.

- **Models to explain the particle injections** (*Li et al., 1998; Sarris et al., 2002*).
  An earthward propagating pulse with constant velocity of westward E and corr. B.

Electric field pulse model

Time varying fields associated with dipolarization in magnetotail, modeled as an electromagnetic pulse (*Li et al., 1998; Sarris et al., 2002*):

- Perturbed fields propagate from tail toward the Earth;
- Time-dependent Gaussian pulse with azimuthal E;
- E propagates radially inward at a decreasing velocity;
- decreases away from midnight.

Time-dependent B from the pulse is calculated by Faraday's law.

In spherical coordinates (r, θ, φ):
$$E_\phi = -E_0 \left(1 + c_1 \cos(\phi - \phi_0)\right)^p \exp\left(-\xi^2\right),$$

$$\xi = \left[r - r_i + v(r)(t - t_a)\right]/d$$

- location of the pulse maximum, r_I determines pulse arrival time

$$v(r) = a + br$$

- pulse front velocity, d - width of pulse, c_1, p describe LT dependence of E amplitude, largest at ϕ_0,

$$t_a = \left(c_2 R_E / v_a\right)\left(1 - \cos(\phi - \phi_0)\right)$$

- delay of pulse from ϕ_0 to other LTs, c_2 - delay magnitude, v_a - longitudinal propagation speed

Electric and magnetic fields in pulse model
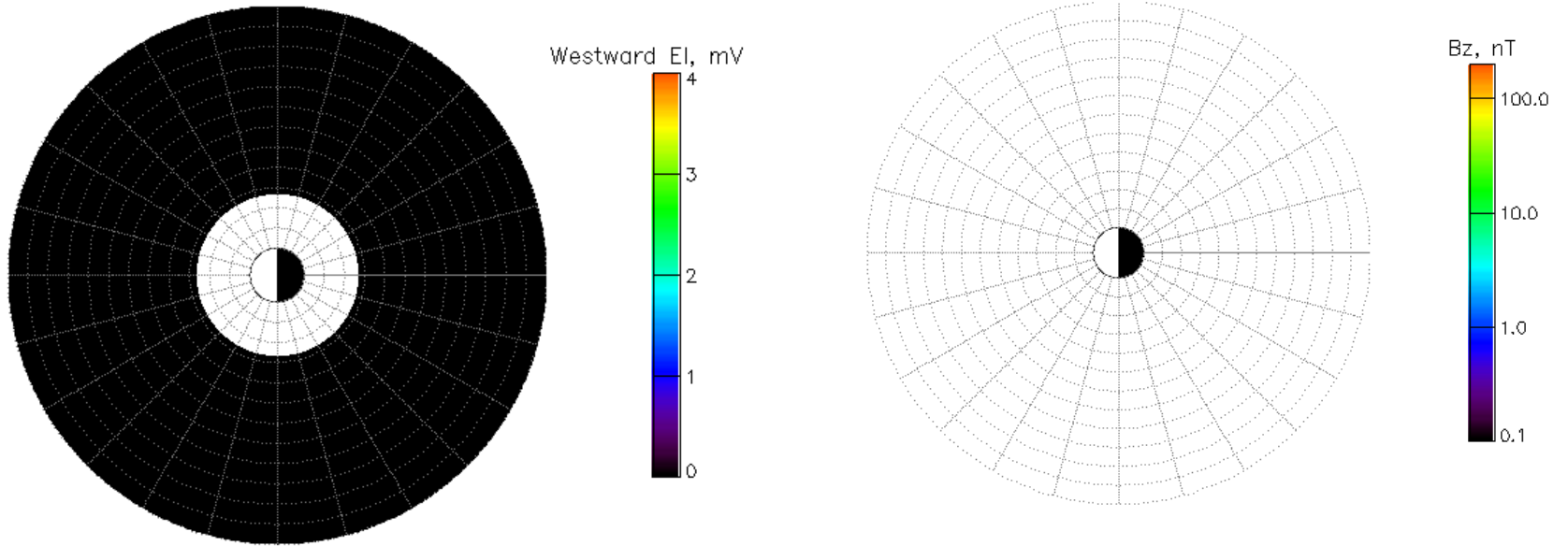
October 21-23, 2001 storm: Addition of pulsed electromagnetic field
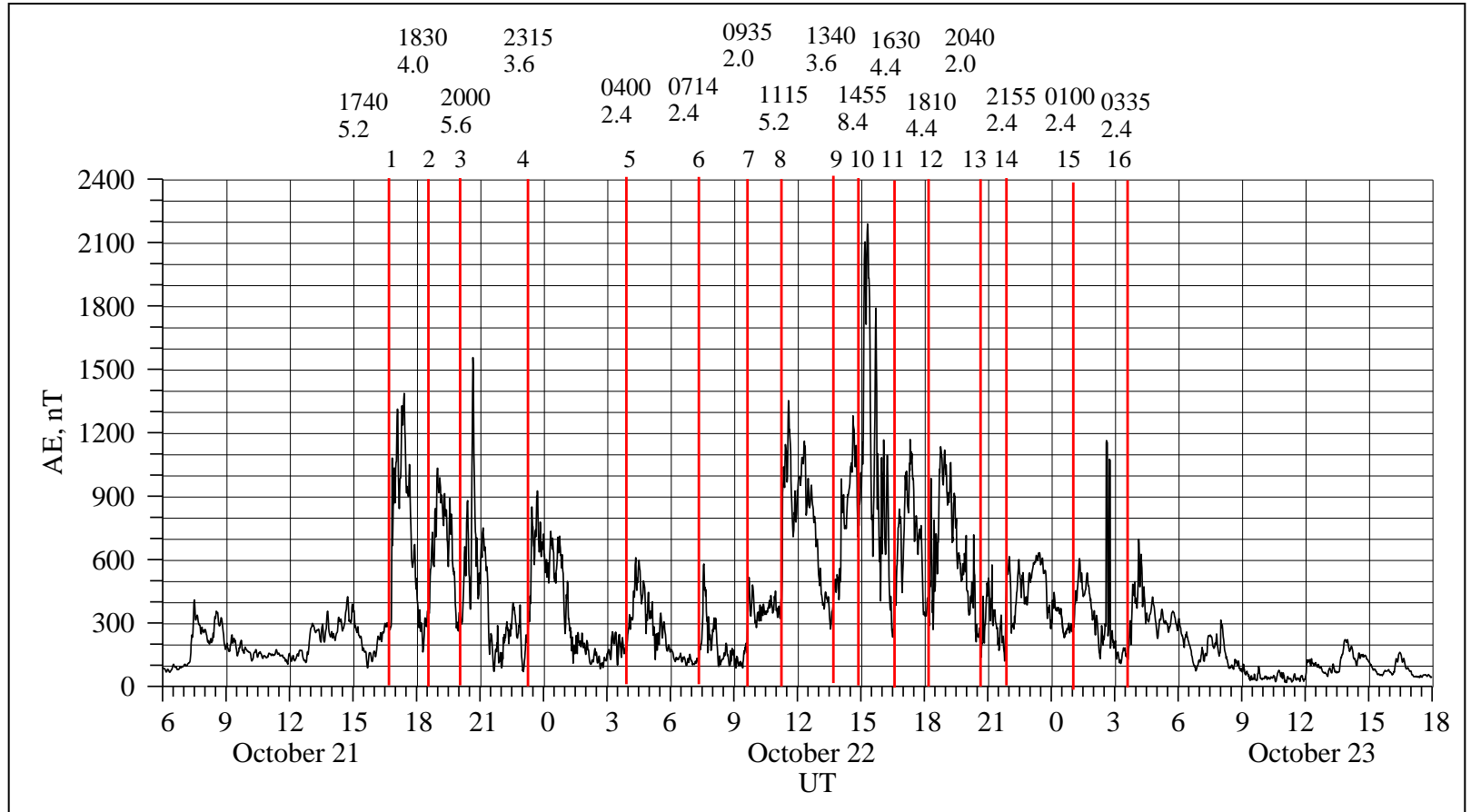
October 21-23, 2001 storm: Pulsed e-m field

20-80 keV

80-300 keV

e_den, keV/m3

10^8

10^6

10^4

10^2

10^0

Dst observed, nT

0

-100

-200

-300

0 6 12 18 0 6 12 18 0 6 12 18 0 6 12 18 24

Oct 20   Oct 21   Oct 22   Oct 23
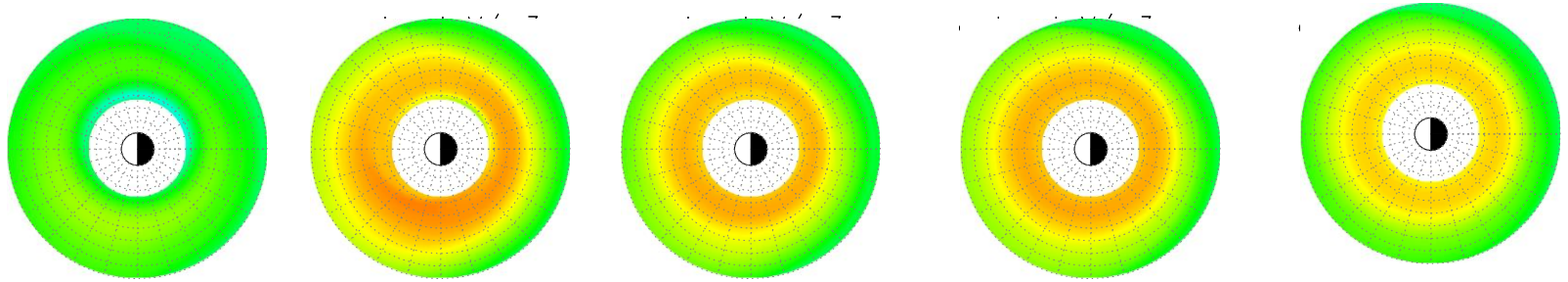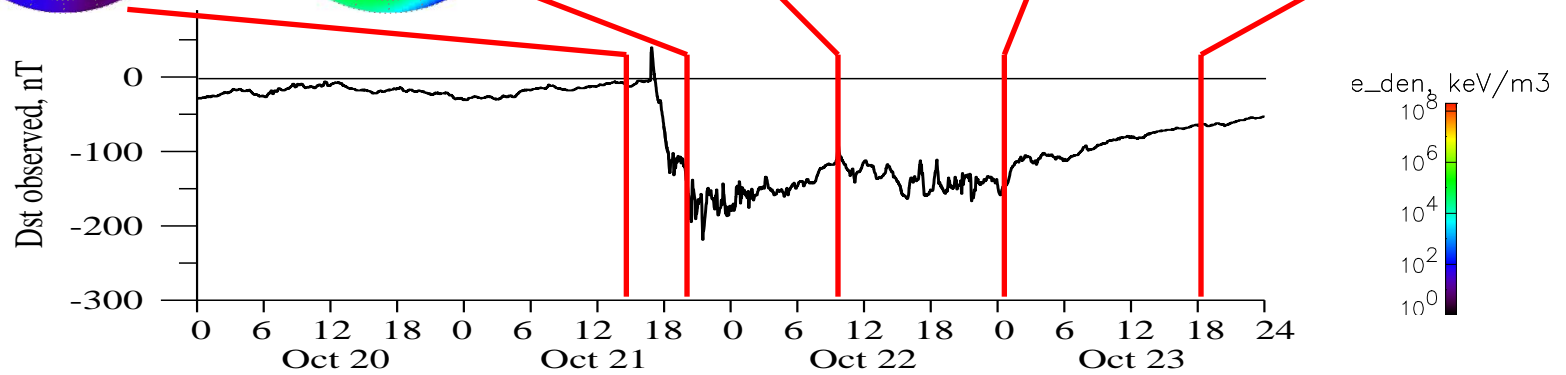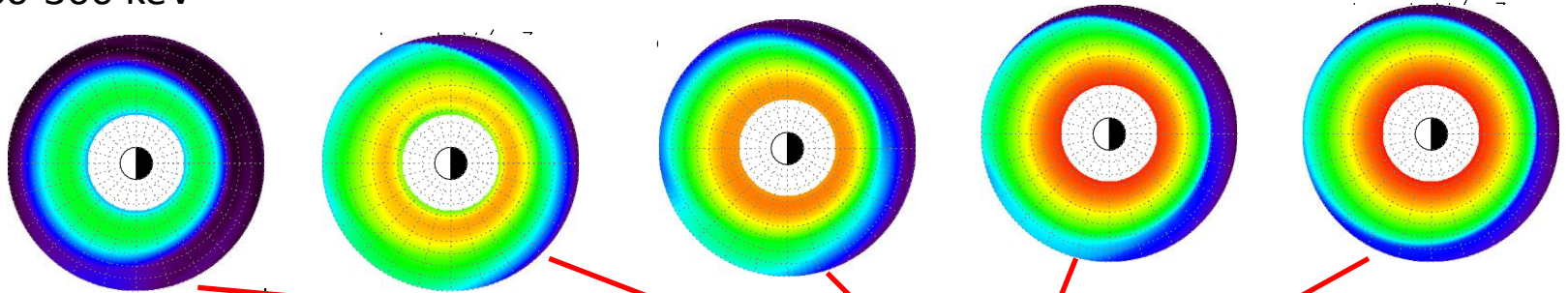
Role of substorm associated electromagnetic pulses in the ring current formation during May 2-4, 1998 storm
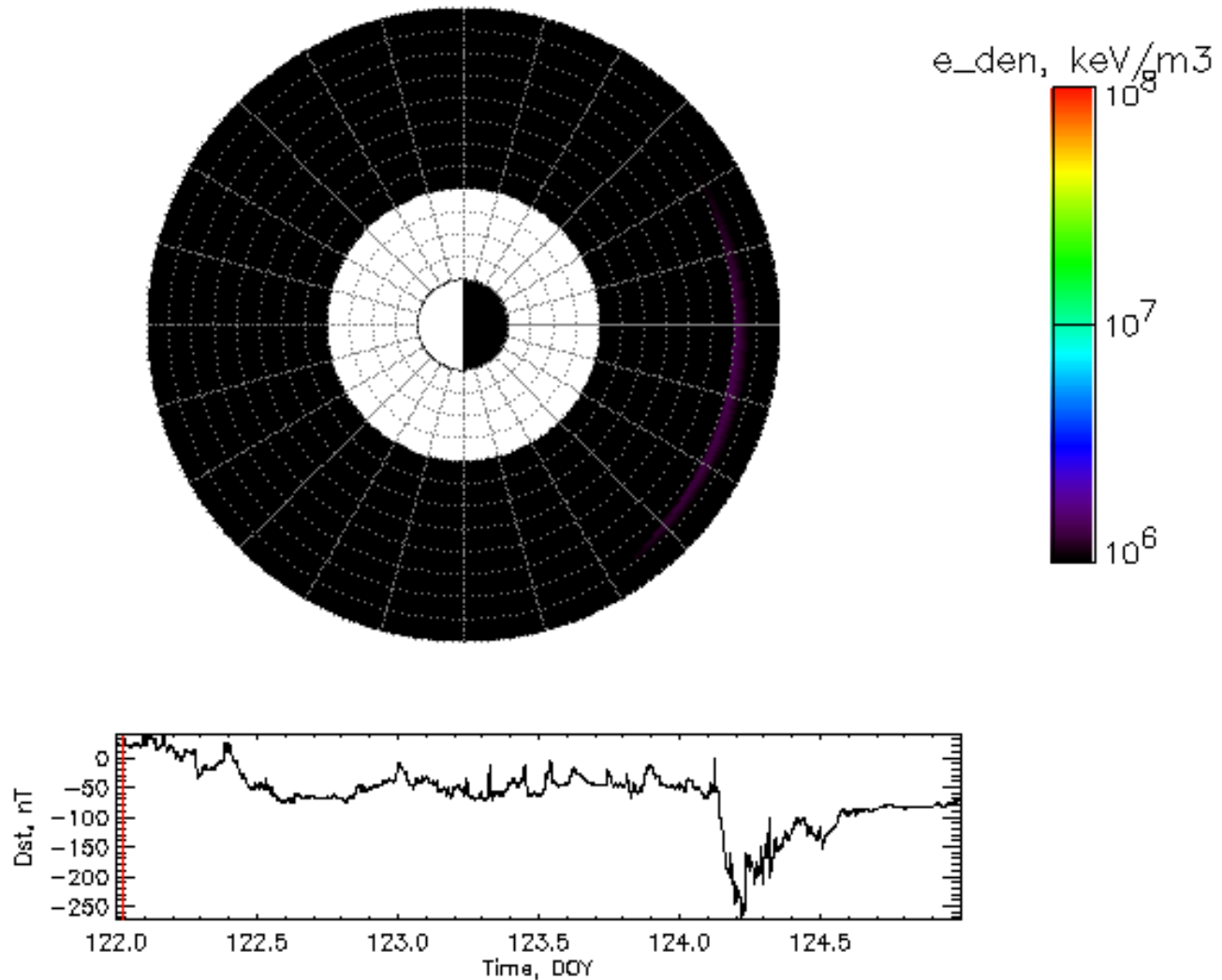
Q1: What are the common/uncommon assumptions we make and should they be revisited?

Magnetic Fields: Self-consistency

Including self-consistent magnetic field

- Obtain parallel pressure and perpendicular pressure from IMPTAM

$$P_\parallel = \int mv^2 f \cos^2 \alpha \, dp, \quad P_\perp = \int \frac{1}{2} mv^2 f \sin^2 \alpha \, dp, \quad dp = m^3 v^2 d\Omega dv$$

- Calculate the current perpendicular to magnetic field

$$\vec{j}_\perp = \frac{\vec{B}}{B^2} \times \left(\nabla P_\perp + \frac{P_{II} - P_\perp}{B^2} (\vec{B} \cdot \nabla) \vec{B} \right)$$

- Calculate the magnetic field induced by the ring and near-Earth tail currents using the Biot-Savart law

$$B(\vec{r}) = \frac{\mu_0}{4\pi} \int \int \int \frac{\vec{J}_\perp(\vec{r}\,') \times (\vec{r} - \vec{r}\,')}{|\vec{r} - \vec{r}\,'|^3} d^3 r'$$

- Calculated magnetic field is then used in IMPTAM to update the particle trajectories

- The procedure repeated 2 or 3 times, dependent on when the following calculations do not differ from the previous ones

Magnetic storm on July 21-23, 2009

July 21-23, 2009

Smooth southward turning of IMF Bz
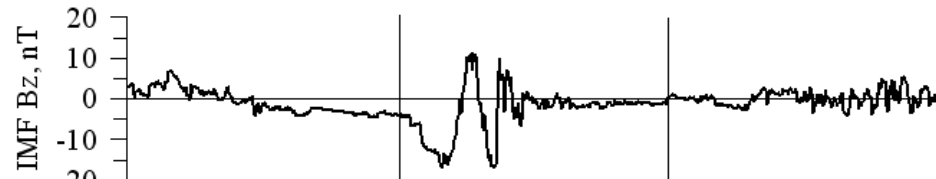
High speed stream

Density peak in front of High Speed stream
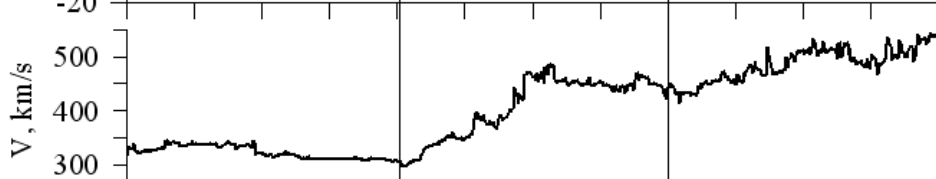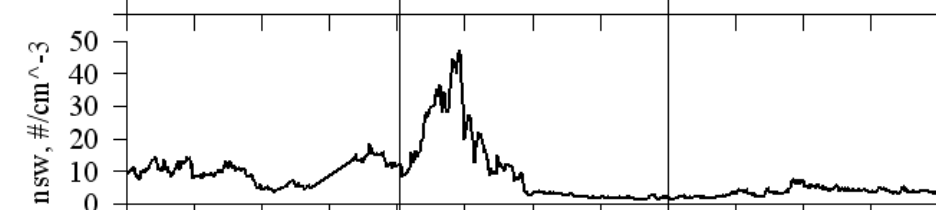
Substorm activity

Small storm
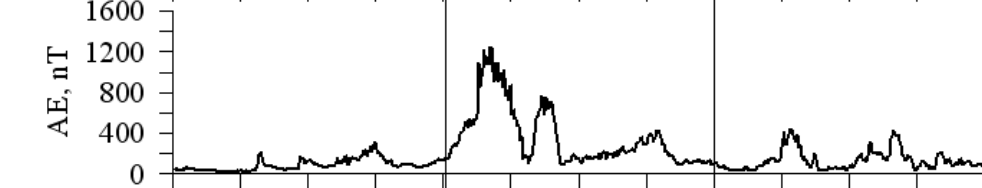
Long recovery
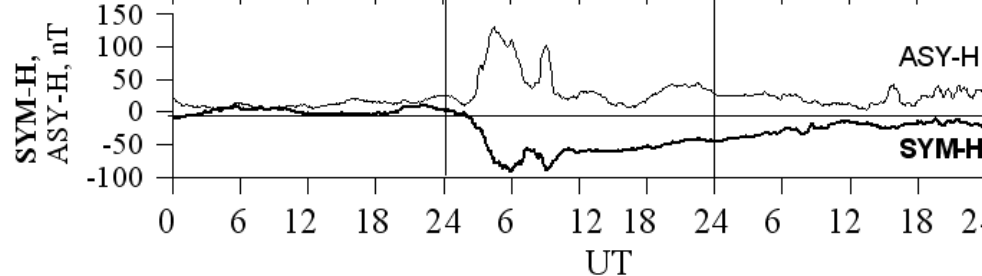
Modeled Dst for July 21-23, 2009 storm
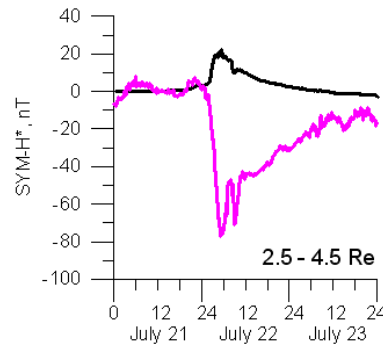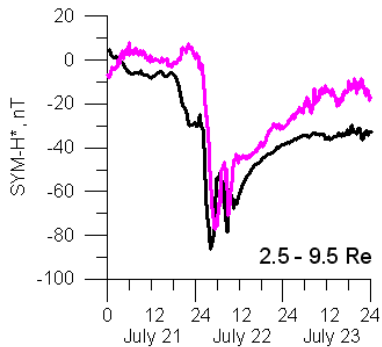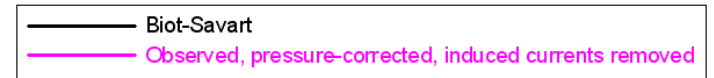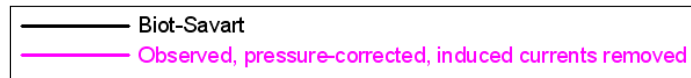## Dip + Boyle + Tsyganenko and Mukai, 2003 at 10 Re

without self-consistent mag. field

with self-consistent mag. field

Storm maximum:
Underestimate of total model SYM-H by 40 nT
Main contribution from 6.5-9.5 Re (tail)

Total model SYM-H comparable with obs
4.5-6.5 Re (ring) no change,
6.5-9.5 Re (tail) overestimate by 40 nT

Modeled Dst for July 21-23, 2009 storm
Dip + T96 + Boyle + Tsyganenko and Mukai, 2003 at 10 Re

without self-consistent mag. field   **with self-consistent mag. field**

July 21-23, 2009 CIR storm, dipole + T96 + Boyle + Tsyganenko and Mukai at 10 Re

July 21-23, 2009 CIR storm, dipole + T96 + selfcons + Boyle + Tsyganenko and Mukai at 10 Re
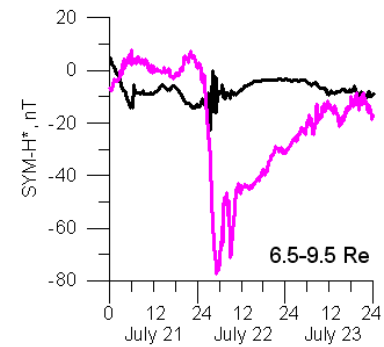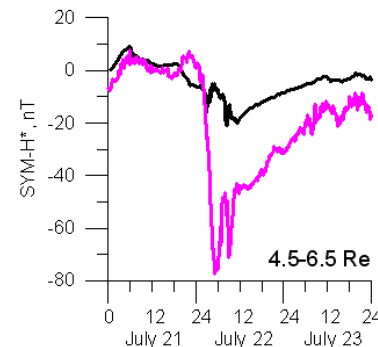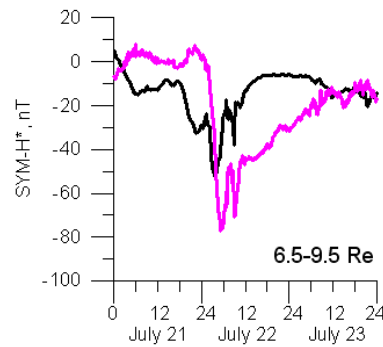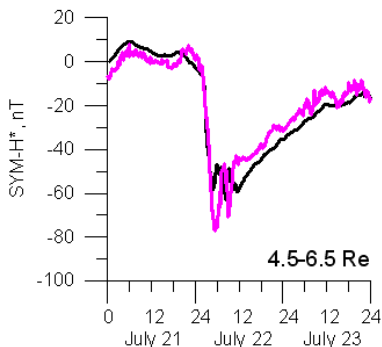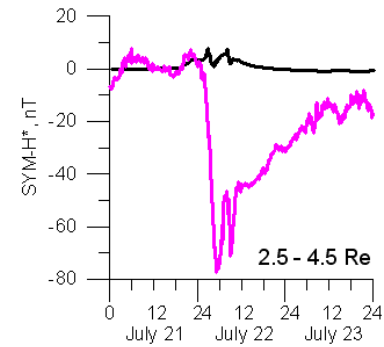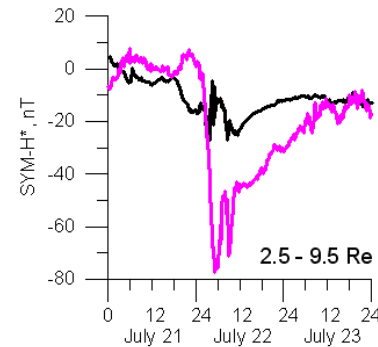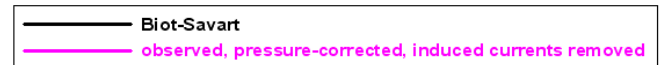
Storm maximum:
Close to observed in total model SYM-H
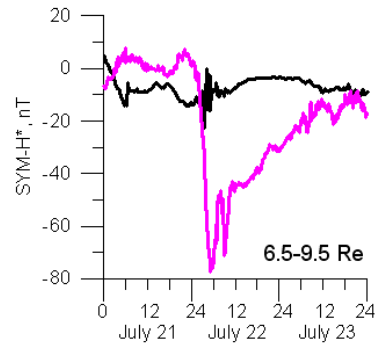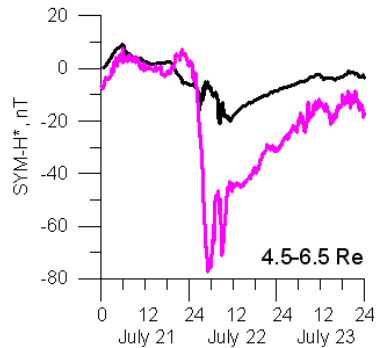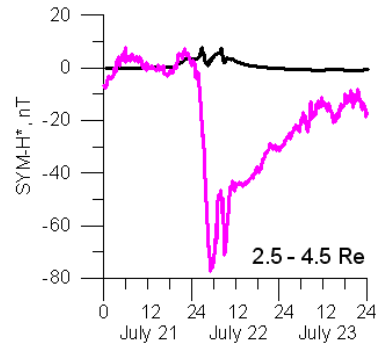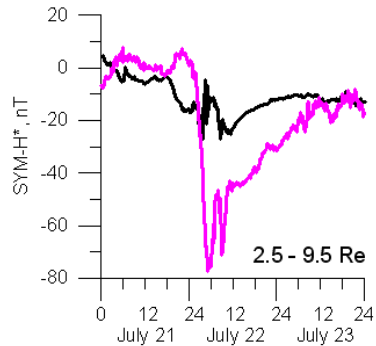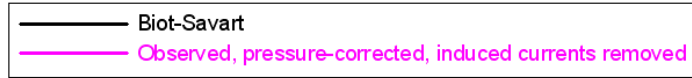Main contribution from 4.5-6.5 Re (ring)

Increase in underestimate of total model
SYM-H by 60 nT
Main contribution from 4.5-6.5 Re (ring)

Modeled Dst for July 21-23, 2009 storm
Dip + T96 + Boyle + Tsyganenko and Mukai, 2003 at 10 Re
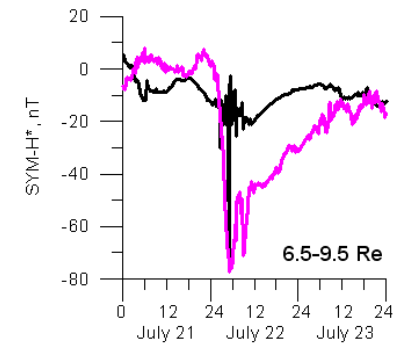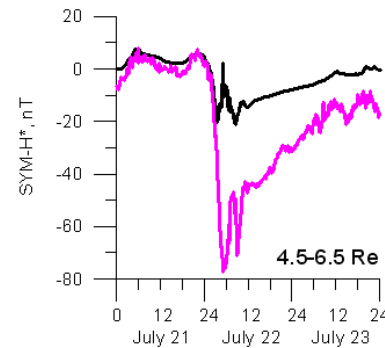
with self-consistent mag. field

T96 RC removed

Modeled Dst for July 21-23, 2009 storm
Dip + T96 + Boyle + Tsyganenko and Mukai, 2003 at 10 Re

with self-consistent mag. field

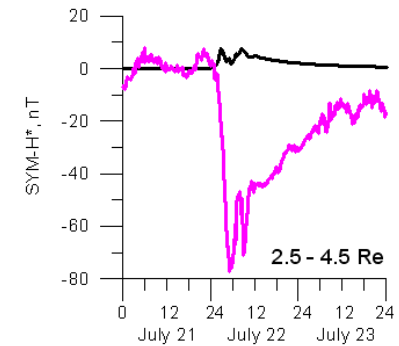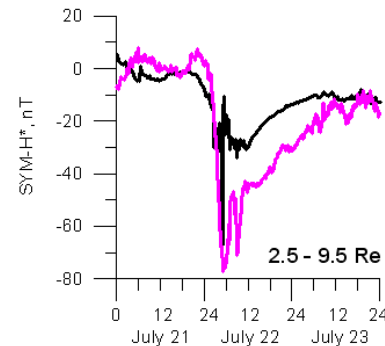## T96 RC and TC removed
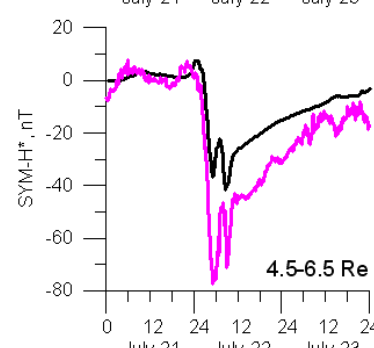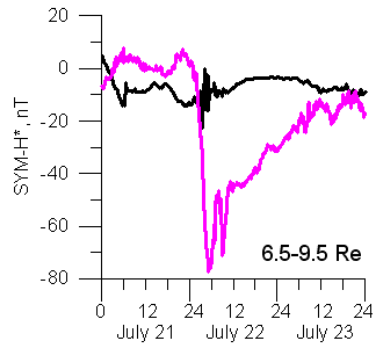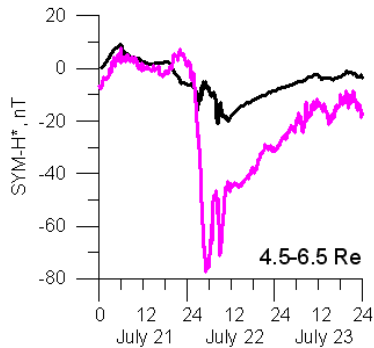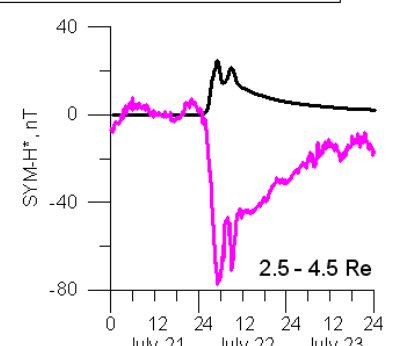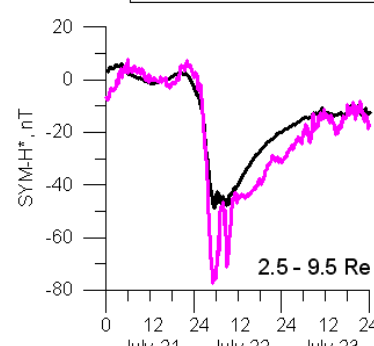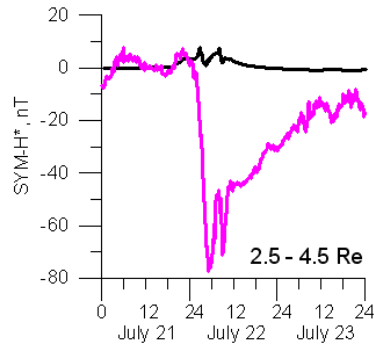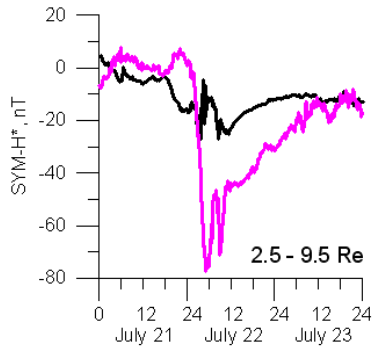
Summary (2)

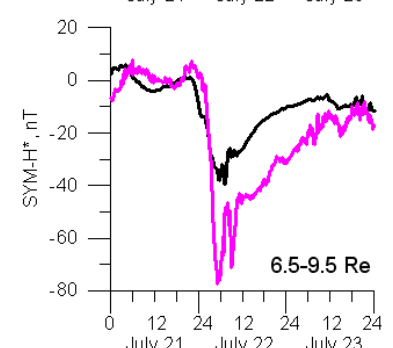1. Including **self-consistent magnetic field** when modeling inner magnetosphere **in dipole background** magnetic field and modeling **in T96 magnetic field** model give comparable results

Can we just use realistic magnetic field models and not include self-consistency?

2. Including self-consistent magnetic field when modeling with T96 background magnetic field model but with T96 ring and tail currents removed

Possible way to include self-consistency to realistic magnetic field models?

Q1: What are the common/uncommon assumptions we make and should they be revisited?

Ion Composition

Ring current energy density and total energy measured by Polar CAMMICE/MICS
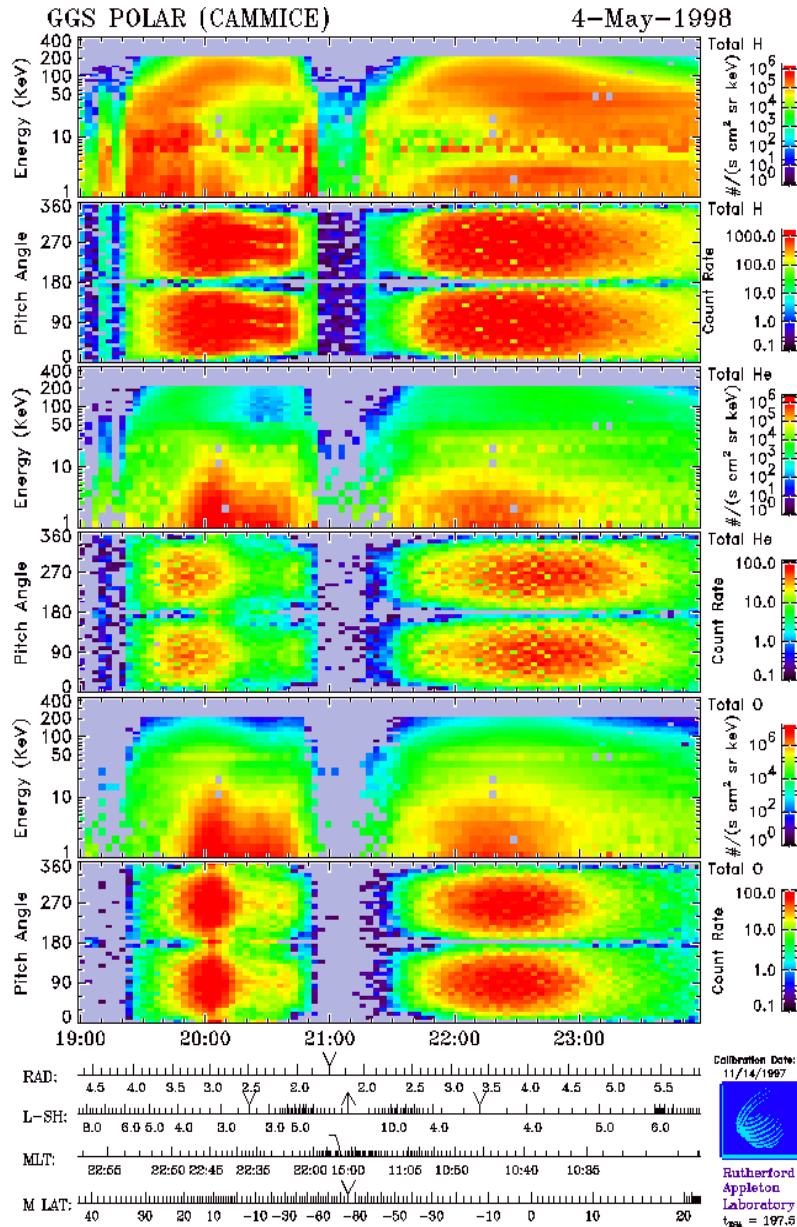
Polar orbit, years 1996-1998

- 1.8x9 Re elliptical, 86 deg inclination,
- 18 hours period, apogee over north polar reg.,
- spin axis normal to orbit plane,
- ions (H+, He+, He++, O+,O++) of 1-200 keV

Energy density of ring current particles

$$w(L) = 2\pi\sqrt{2mq}\int_0^\infty dE\sqrt{E}\,j(E,L),$$

m - particle mass, q - particle charge state,
E - energy, j - measured particle flux

Total ring current energy

$$W_{RC} = \int_V w(L)\,dV,$$

$$dV = 2R_E^3 L^2\sqrt{1-\frac{1}{L}}\left(\frac{1}{7L^3}+\frac{6}{35L^2}+\frac{8}{35L}+\frac{16}{35}\right)dLd\phi$$

ϕ - local time

Contributions to ring current energy from different energy ranges for ion species: 27 storm statistics (1)
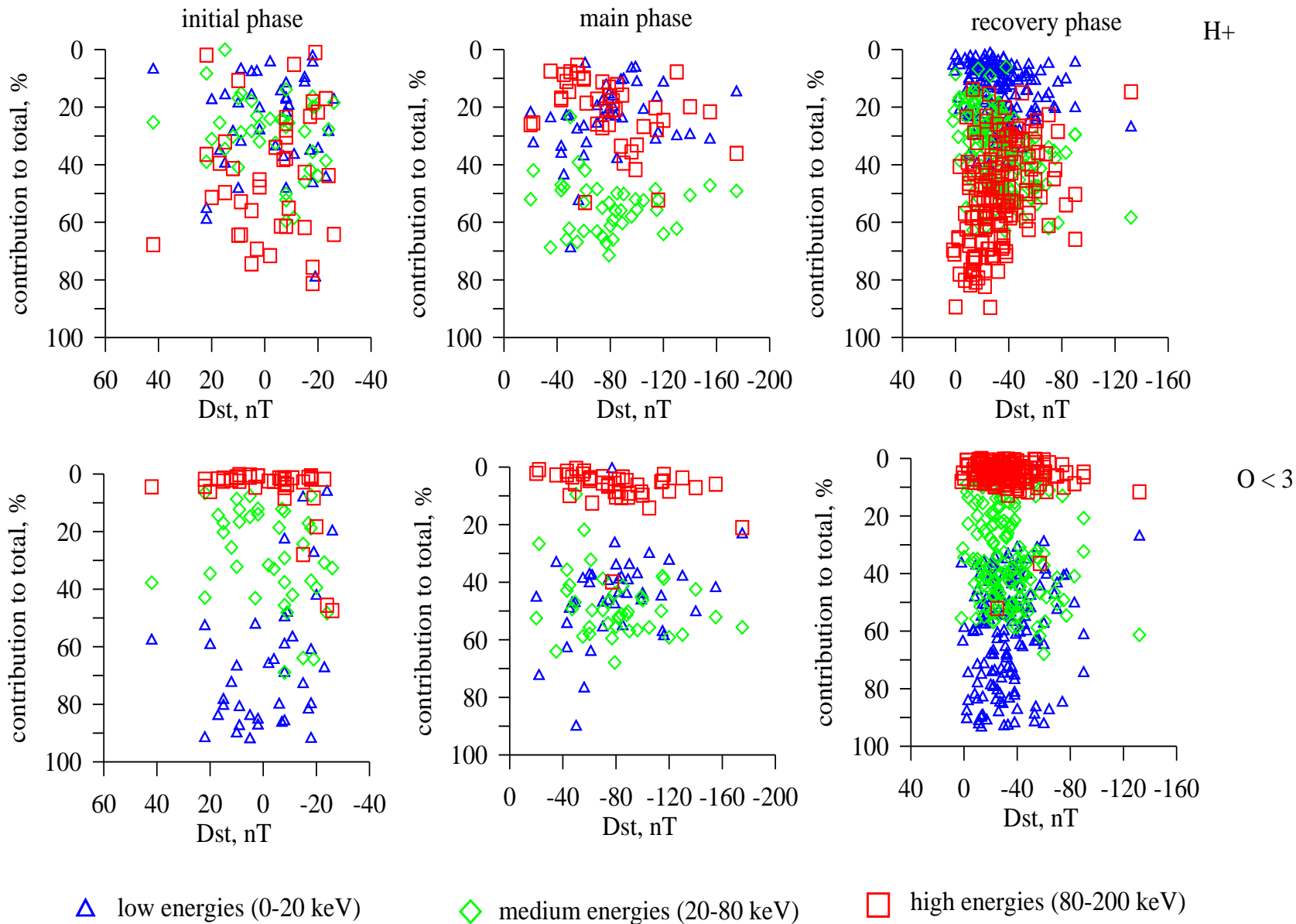
Contributions to ring current energy from different energy ranges for ion species: 27 storm statistics (2)
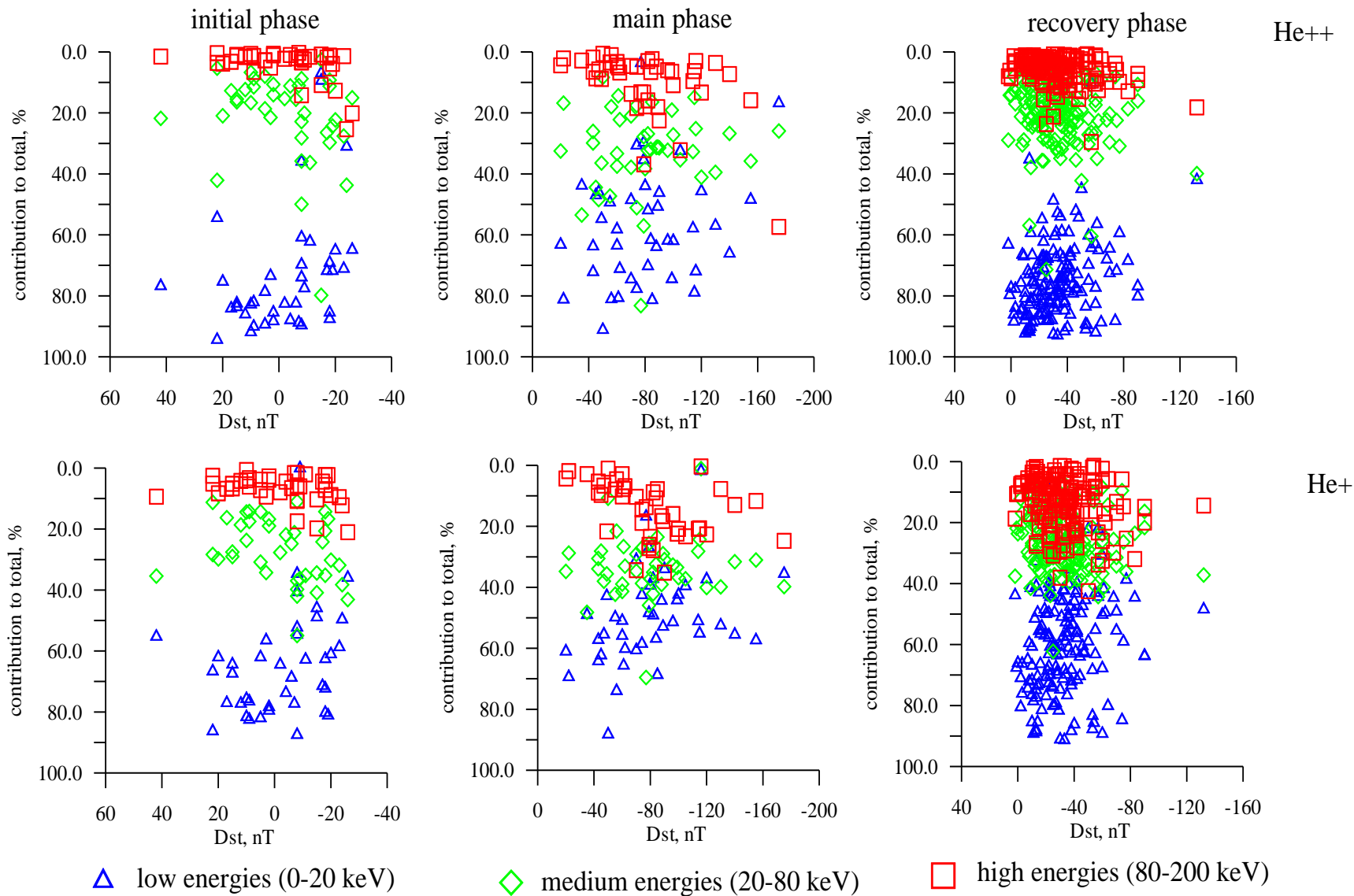
Contributions to ring current energy from ion species: Storm statistics
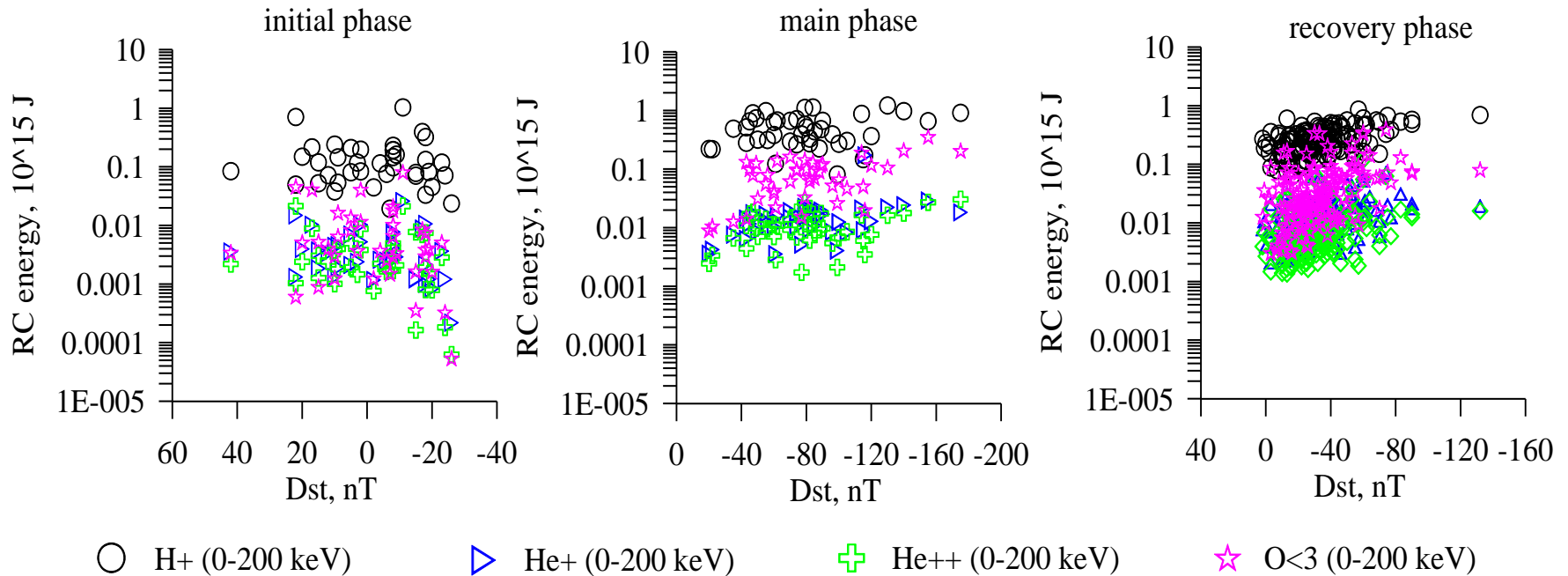
Initial phase: almost similar contributions (10^12 J) from ion species (He+,++, O+,++), no dependence on Dst

Main phase: larger contribution from He+ and He++ (10^13 J), O+,++ contribution increase up to several 10^14 J, increase with Dst decrease

Recovery phase: order of difference between He+,++ and O+,++ contributions (10^12-10^13 and 10^13-10^14), decrease with Dst increase

Advances in IMPTAM for electrons

Magnetic field model: *Tsyganenko* T96 (Dst, Psw, IMF By and Bz)

Electric field model: *Boyle et al.* (1997) (Vsw, IMF B, By, Bz)

Boundary conditions at 10 Re: newly developed empirical model for electron number density and temperature in the plasma sheet based on THEMIS observations (instead of *Tsyganenko and Mukai* (2003) model for ions) (Vsw, IMF Bz,Nsw)

Radial diffusion with diffusion coefficients D_{LL} (*Brautigam and Albert,* 2000)

$$D_{LL} = 10^{0.056Kp - 9.325} L^{10}$$

Losses:

Parameterization of the electron lifetimes due to interactions with chorus waves [*Orlova and Shprits,* 2014] and **due to interactions with hiss waves** [*Orlova et al.,* 2014]: polynomial expressions with coefficients dependent on energy, radial distance, MLT sector and Kp.

References:

Ganushkina, et al., Nowcast model for low-energy electrons in the inner magnetosphere, Space Weather, 13, doi:10.1002/2014SW001098, 2015.

Ganushkina et al., Low energy electrons (5-50 keV) in the inner magnetosphere, J. Geophys. Res., 119, doi:10.1002/2013JA019304, 2014.

Ganushkina, et al., Transport of the plasma sheet electrons to the geostationary distances, J. Geophys. Res.: Space Physics, 118, doi:10.1029/2012JA017923, 2013.

Boundary conditions in the plasma sheet for modeling of keV electrons

Near-Earth plasma sheet is the source for keV electrons in the inner magnetosphere.
In the near-Earth plasma sheet, continuous measurements of plasma sheet electrons are not available, in contrast to geostationary orbit.

No solar wind driven empirical relations for electron fluxes or moments of electron distribution function which can be used easily for radiation belt modeling.

Our previous studies [*Ganushkina et al.*, 2013, 2014]:
we set the model **boundary at 10 R_E** and use the **kappa electron distribution** function.
Parameters of the kappa distribution function: **number density n and temperature T** in the plasma sheet given by the empirical model derived from Geotail data by TM03 *Tsyganenko and Mukai* [2003]. The **electron n is assumed to be the same as that for ions** in the TM03 model, but **Te/Ti = 0.2** is taken into account (*Wang et al.,* 2012).

Applying this model for boundary conditions has a number of **limitations**:

(1) Model was derived from **Geotail data for ions** (limited detector energy range <40keV).

(2) ratio **Te/Ti can vary** during disturbed conditions.

(3) at distances closer than 10 Re, the correlation between Ti and Te might not exist at all and no certain ratio can be determined (*Runov et al.,* 2015).

Revision of boundary conditions in the plasma sheet using THEMIS data

THEMIS data for ions and electrons used:
ESA (a few eV up to 25 (30) keV) and **SST** (25 keV- few MeVs).

Data for **storm periods**: All the periods with SYM-H<-50nT and one day before and one day after these periods for 2007-2013. The quiet periods before the storms are also in our database.

Then we computed the **plasma moments** using last calibration procedures. After synchronization of the solar wind data with THEMIS plasma moments we got ~66,000 datapoints at 1.5 min resoluton.
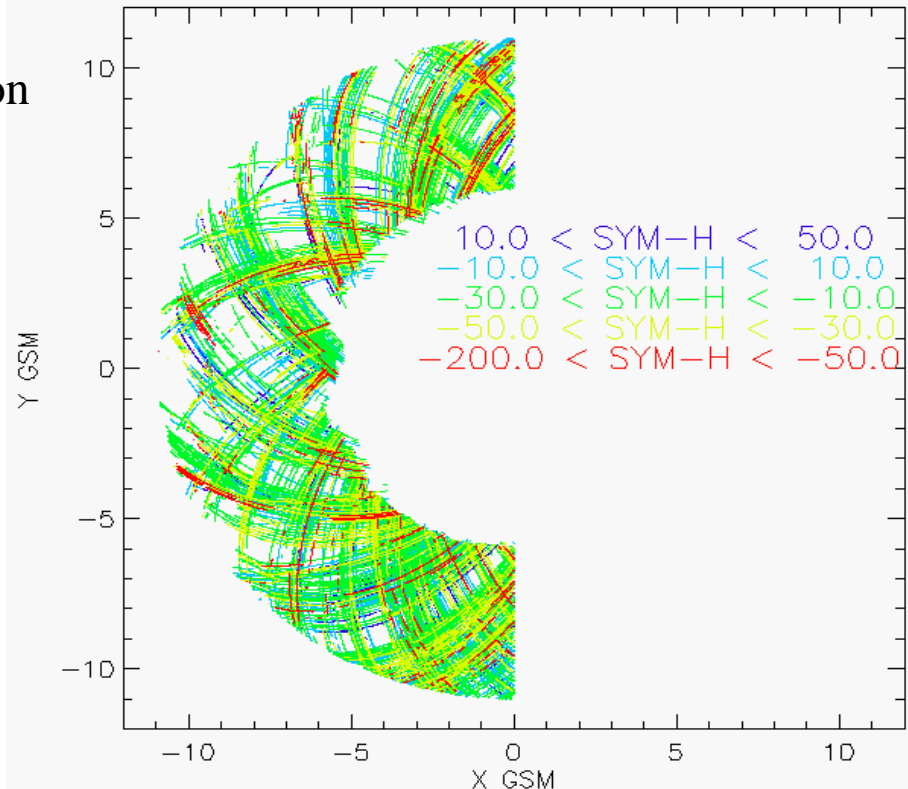
Model for electron temperature at 6-11 R_e based on Cluster and THEMIS data: Empirical relations

Every point in the inner magnetosphere is defined by two normalized coordinates $\phi*$ and $R*$. The angle

$$\phi* = \frac{2}{\pi} \arctan\left(\frac{-Y_{GSM}}{X_{GSM}}\right) \text{ and } R* \text{ is the geocentric distance normalized by } 10\ R_E.$$

The number density in the plasma sheet (*Nps*) is given in cm^{-3} as follows:

$$N_{ps} = 0.2579 - 0.1148\phi^* - 0.1520\phi^{*2} + \left(0.3094 - 0.1486\phi^*\right)N_{SW}^* + \left(1.187 - 1.104R^*\right)B_S^{*0.715}$$

$$N_{SW}^*(t_0) = \frac{1}{10cm^{-3}5.75h} \int_{t_0-0.33h}^{t_0-6.08h} N_{SW}(t)dt, \ \ B_S^*(t_0) = \frac{1}{2nT5.25h} \int_{t_0-0.33h}^{t_0-6.08h} B_S(t)dt$$

Nsw is the solar wind density and Bs is the sourthward IMF Bz.
The temperature in the plasma sheet (*Tps*) is given in keV as follows:

$$T_{ps} = \left[\begin{array}{l} 2.749 - 2.611R^* + 0.6191\phi^* - 0.6271\phi^* R^* + 0.5907\phi^{*2}R^* + \\ + \left(1.918R^* + 1.466\phi^{*2} - 2.224\phi^{*2}R^*\right)V_{SW}^* - 0.3587\phi^* B_S^{*0.513} - 0.6948R^* B_N^{*0.498} \end{array}\right]^2$$

$$V_{SW}^*(t_0) = \frac{1}{400km/s}V_{SW}(t-1.58h), \ \ B_S^*(t_0) = \frac{1}{2nT1.5h} \int_{t_0-0.33h}^{t_0-1.83h} B_S(t)dt, \ \ B_N^*(t_0) = \frac{1}{2nT3.25h} \int_{t_0-0.33h}^{t_0-3.58h} B_N(t)dt$$

Vsw, *Bs*, and *Bn* are solar wind density, southward and northward IMF Bz components

Comparison of temperatures of electrons from THEMIS data and of ions from *Tsyganenko and Mukai* [2003] model

Subset of the data with R=10-10.5 R_E is used.
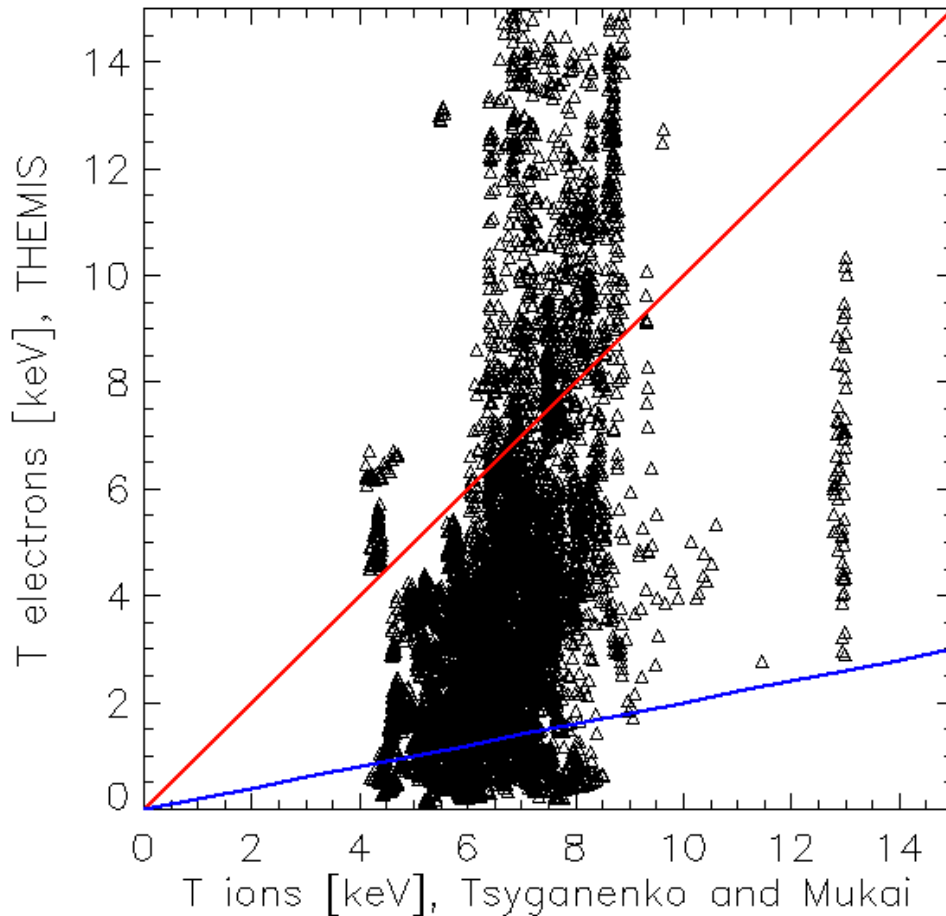
Red line: Te=Ti
Blue line: Te=Ti/5

If the relation Te=Ti/5 would have been valid in this region, the points would be distributed along blue line.
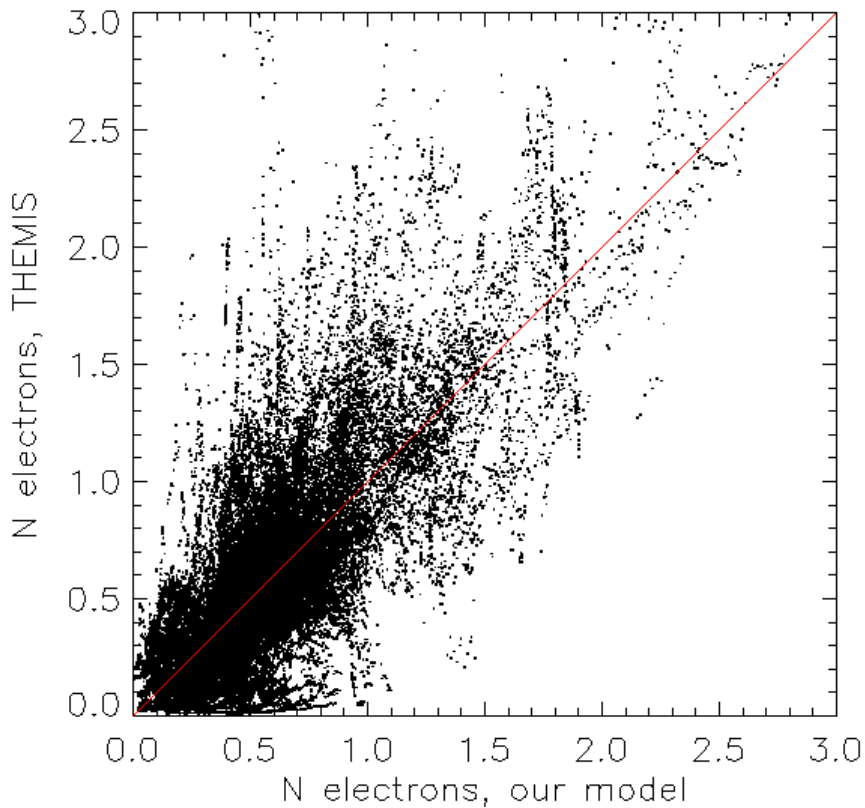
TM03 ion temperature shows **almost no correlation** with measured electron temperature.

Similar to *Runov* [2015] (private communication): there is **no correlation between Ti and Te at geocentric distances closer than R=12Re.**
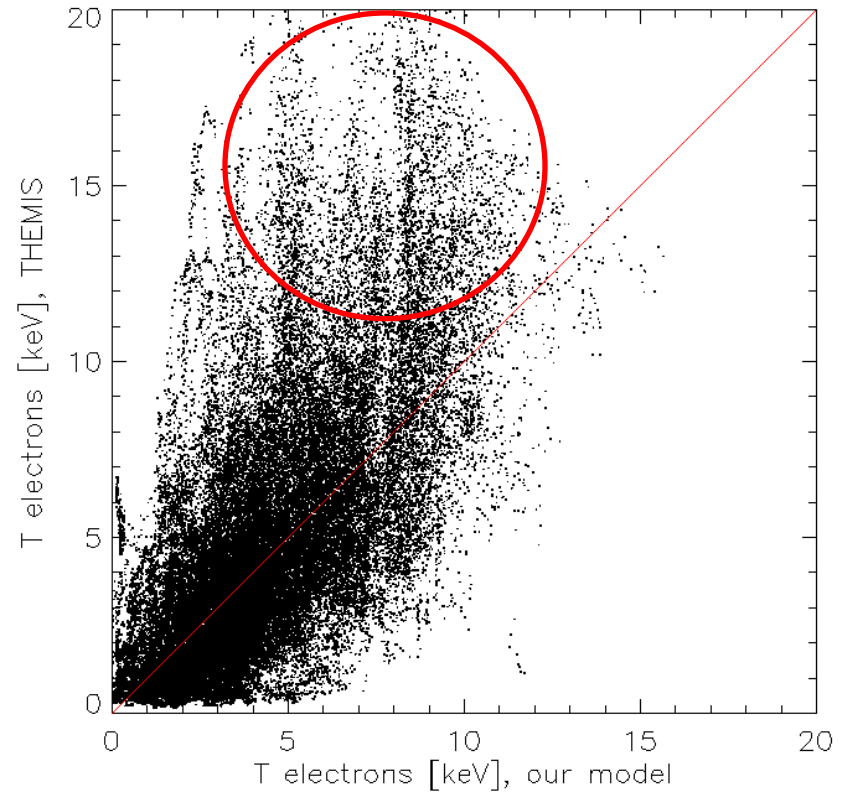
Empirical model for plasma sheet electrons at 6-11 R_e based on THEMIS data: Performance

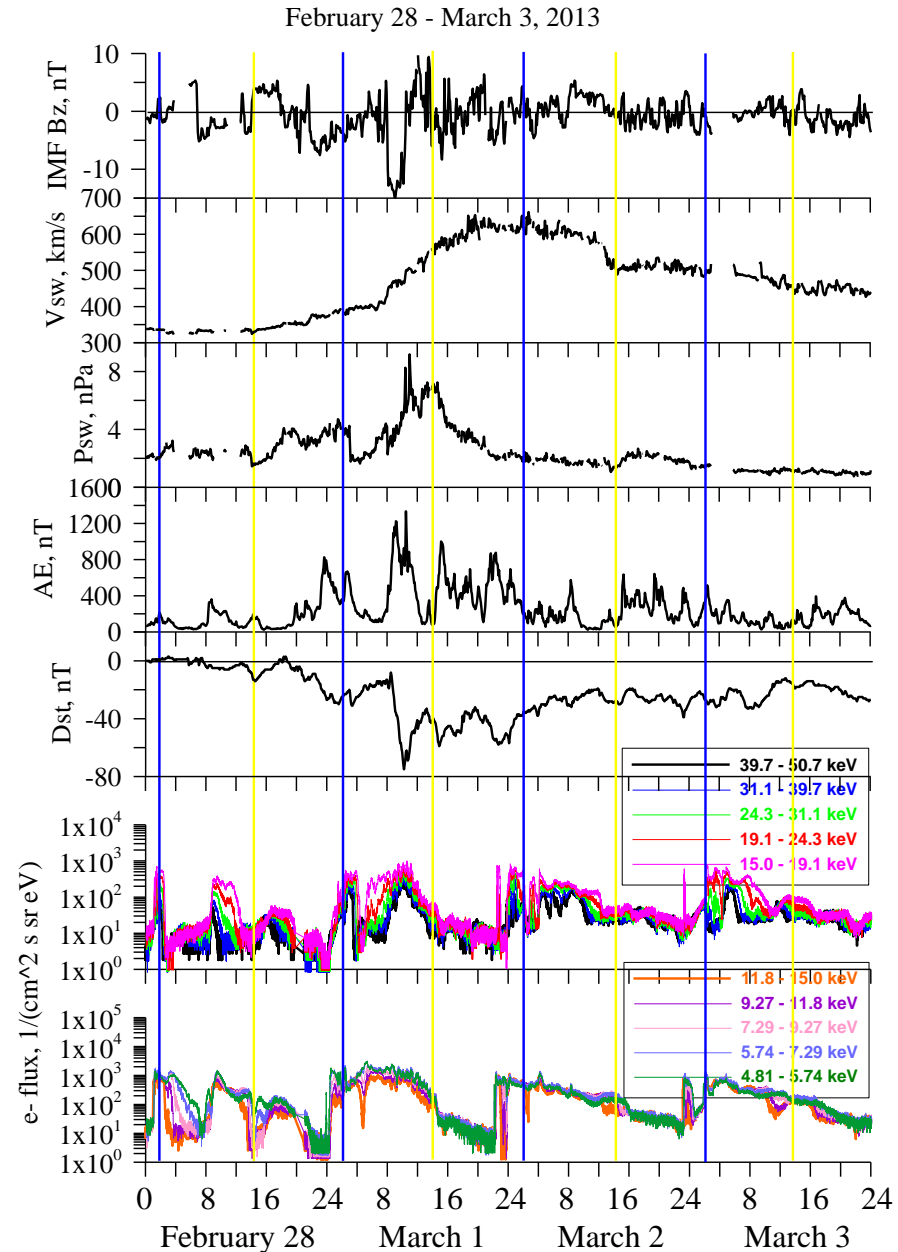Hot plasma carried by BBFs (substorm injections)?
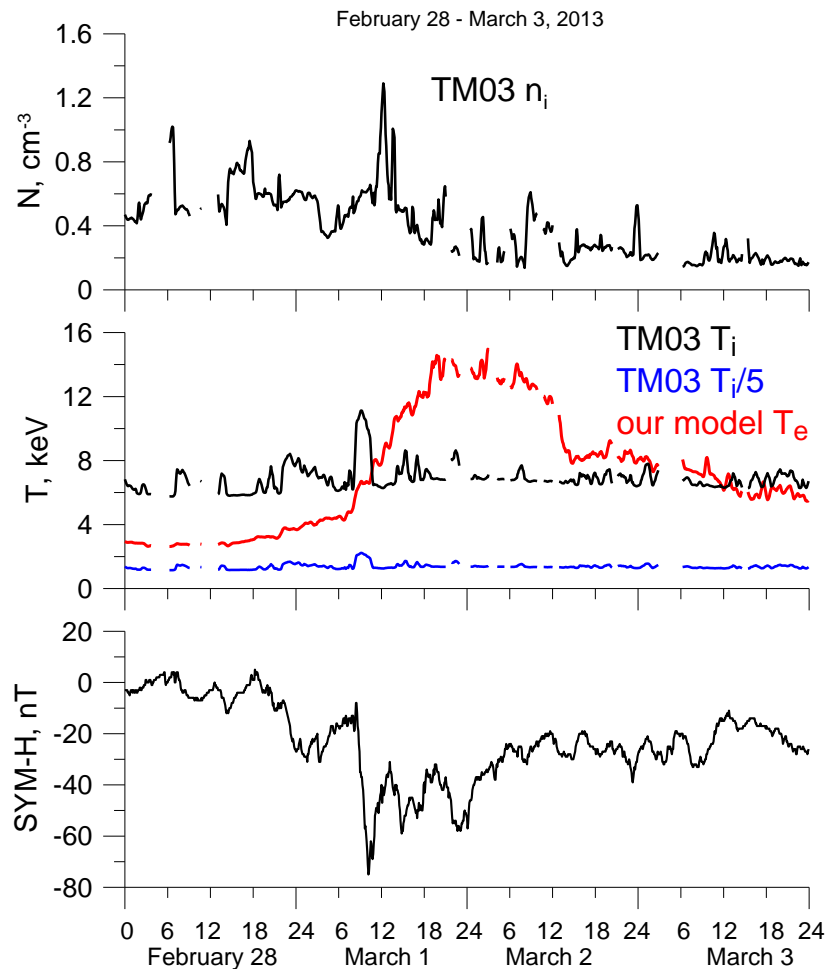
CC=0.76

CC= 0.6559   MAD=2.015   MSD=2.869

AMC 12 CEASE II ESA data

AMC 12 geostationary satellite, CEASE-II instrument contains an Electrostatic Analyzer (ESA) for measuring low energy electron fluxes in 10 channels, 5 - 50 keV.

February 28 - March 3, 2013

Electron fluxes observed by AMC 12 CEASE II ESA instrument for 15-50 keV energies and modeled. No losses are considered.

With *Tsyganenko and Mukai* (2003) boundary conditions
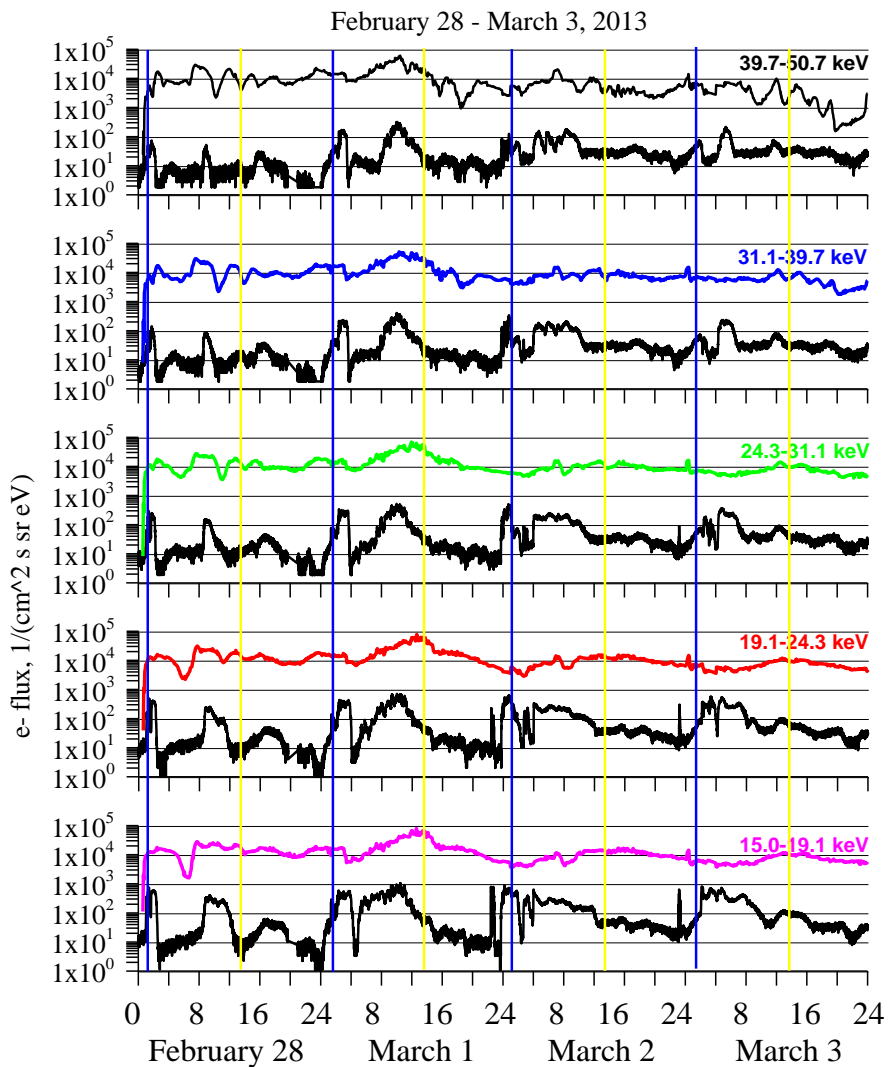
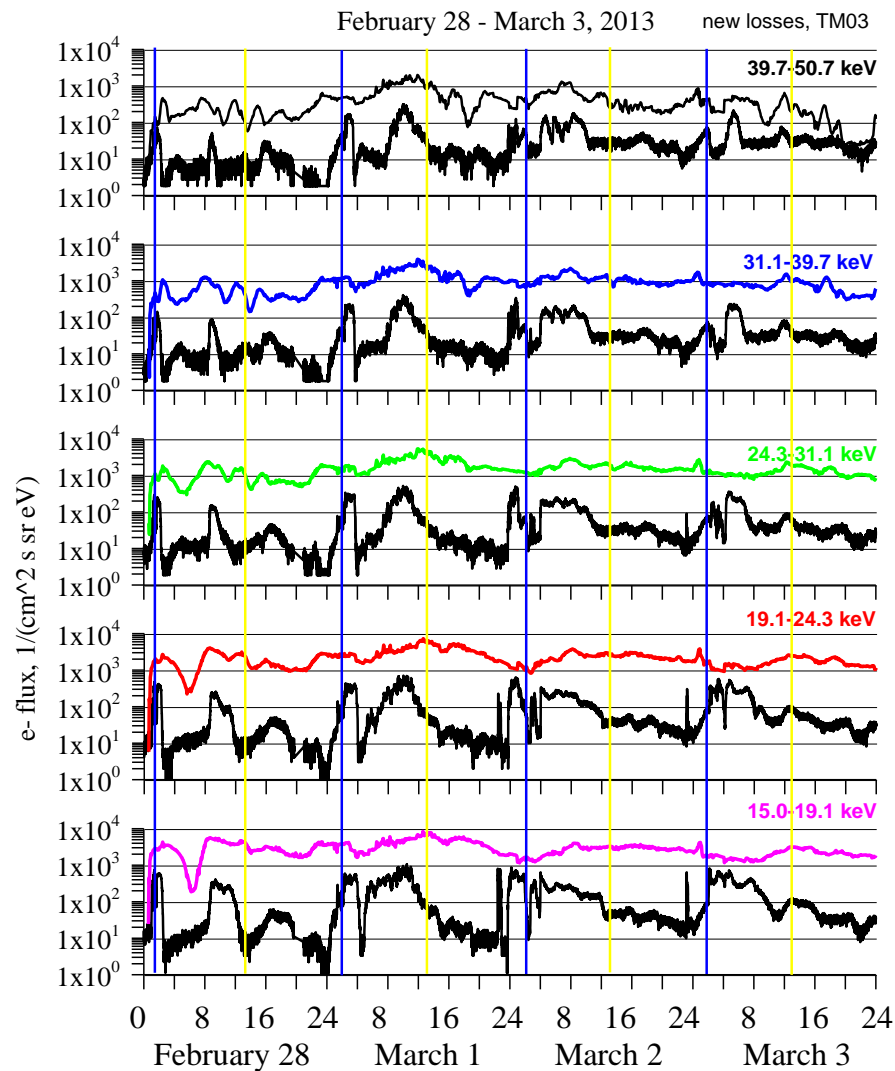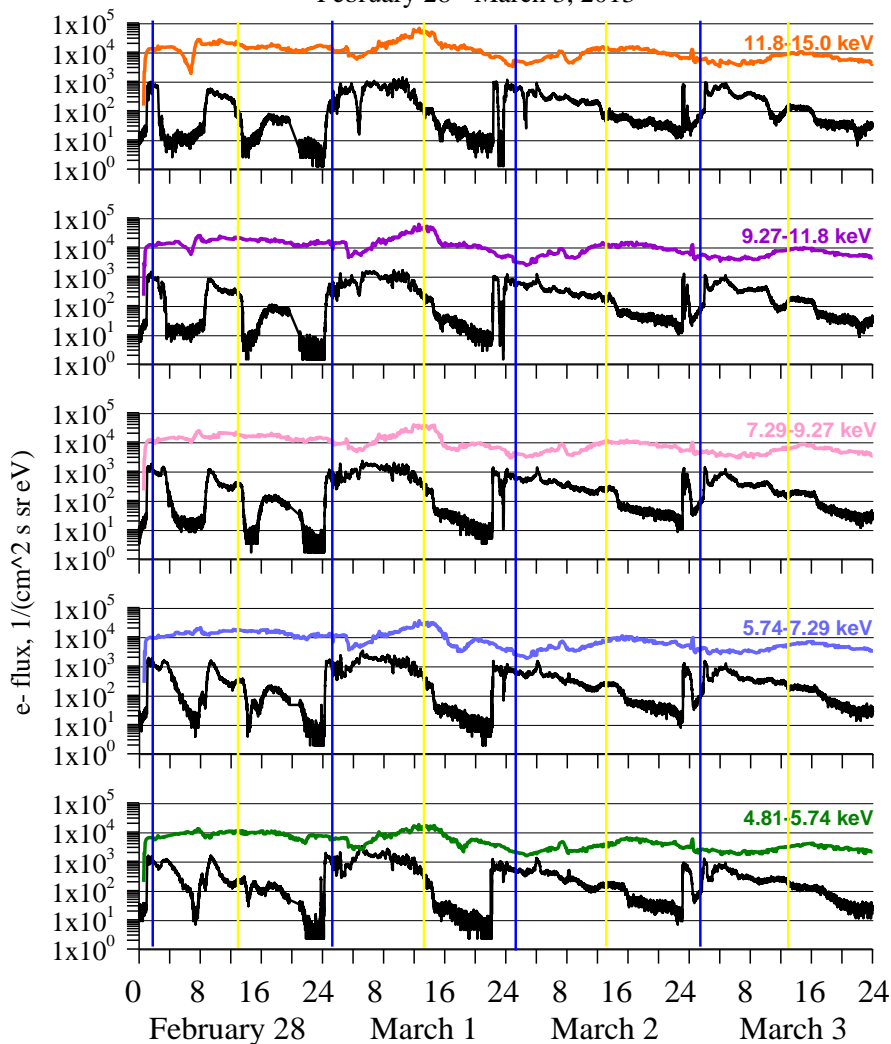with newly developed model for boundary conditions based on THEMIS data

Electron fluxes observed by AMC 12 CEASE II ESA instrument for 5-15 keV energies and modeled. No losses are considered.
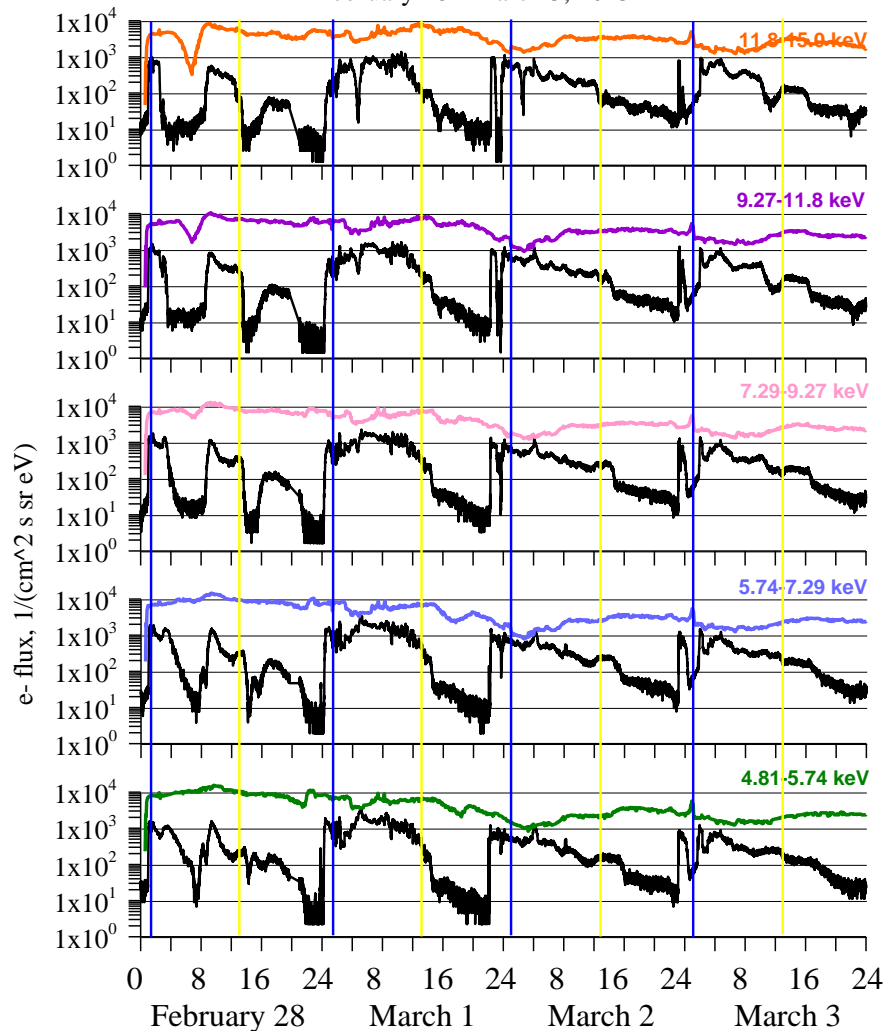
With *Tsyganenko and Mukai* (2003) boundary conditions

with newly developed model for boundary conditions based on THEMIS data

February 28 - March 3, 2013

Electron fluxes observed by AMC 12 CEASE II ESA instrument for 15-50 keV energies and modeled

with **TM03** model and *Chen et al.* **[2005]** electron lifetimes for strong and *Shprits et al.* **[2007]** for weak diffusion

With **THEMIS** model and *Orlova and Shprits* **[2014]** and *Orlova et al.* **[2014]** electron lifetimes

February 28 - March 3, 2013

February 28 - March 3, 2013   new losses, TM03
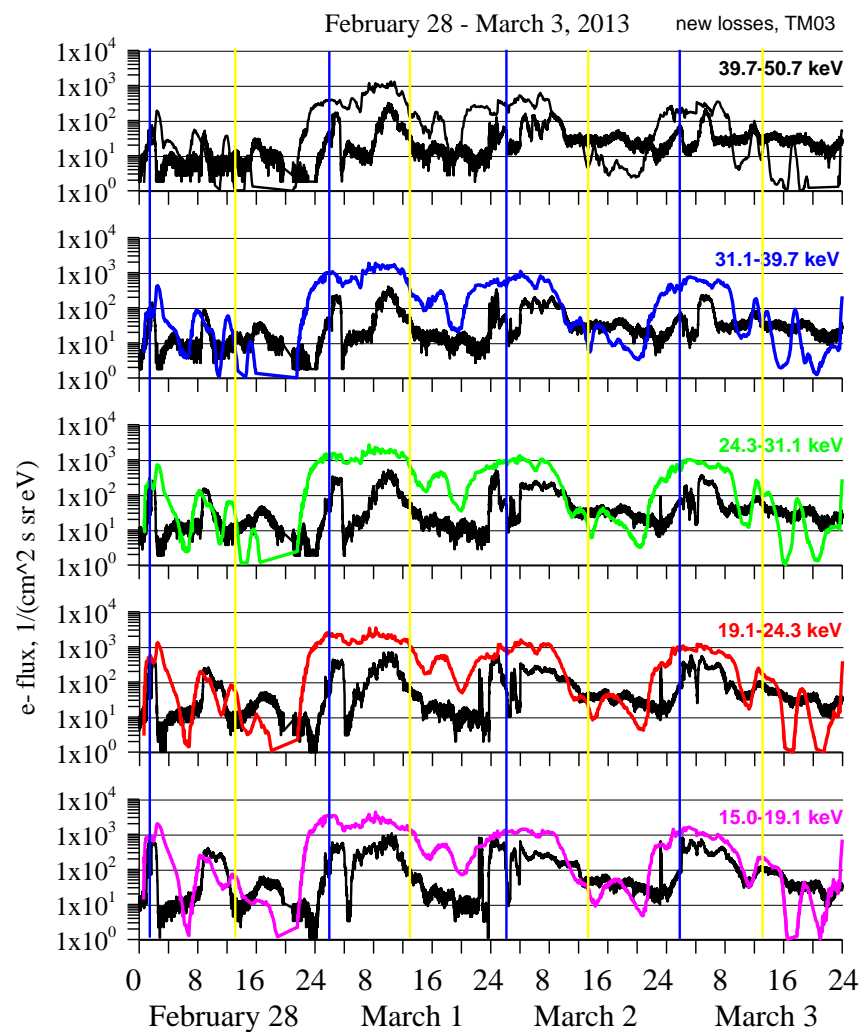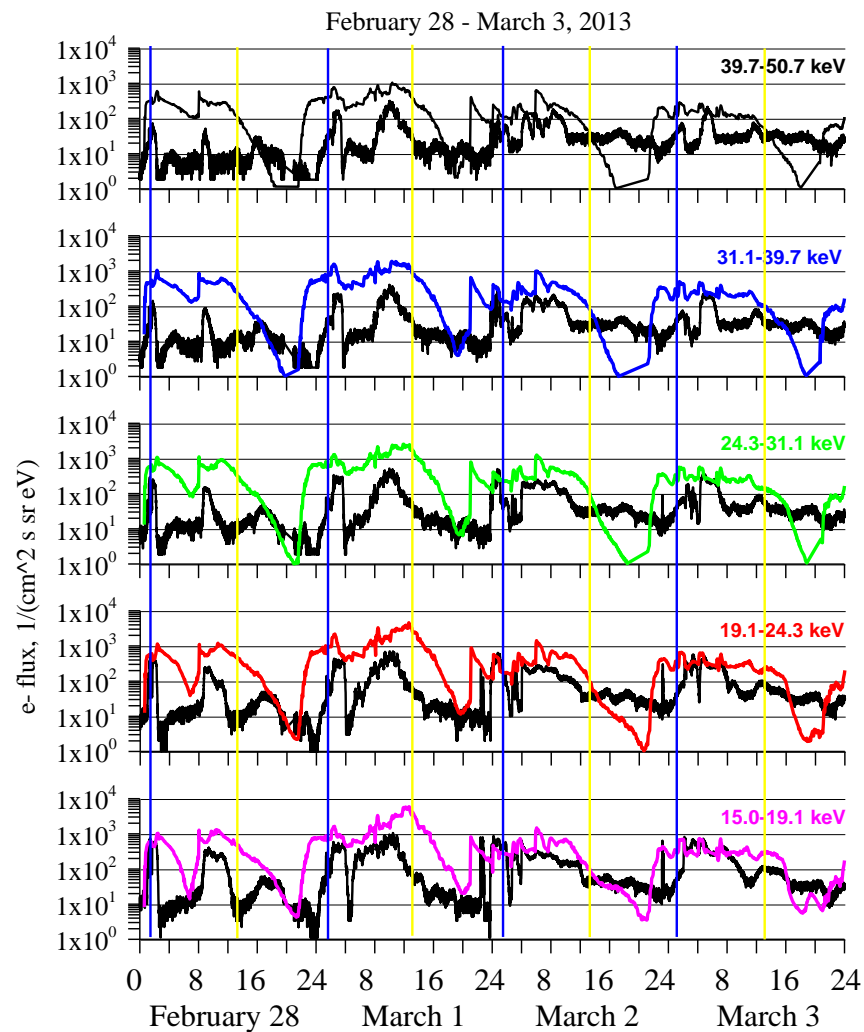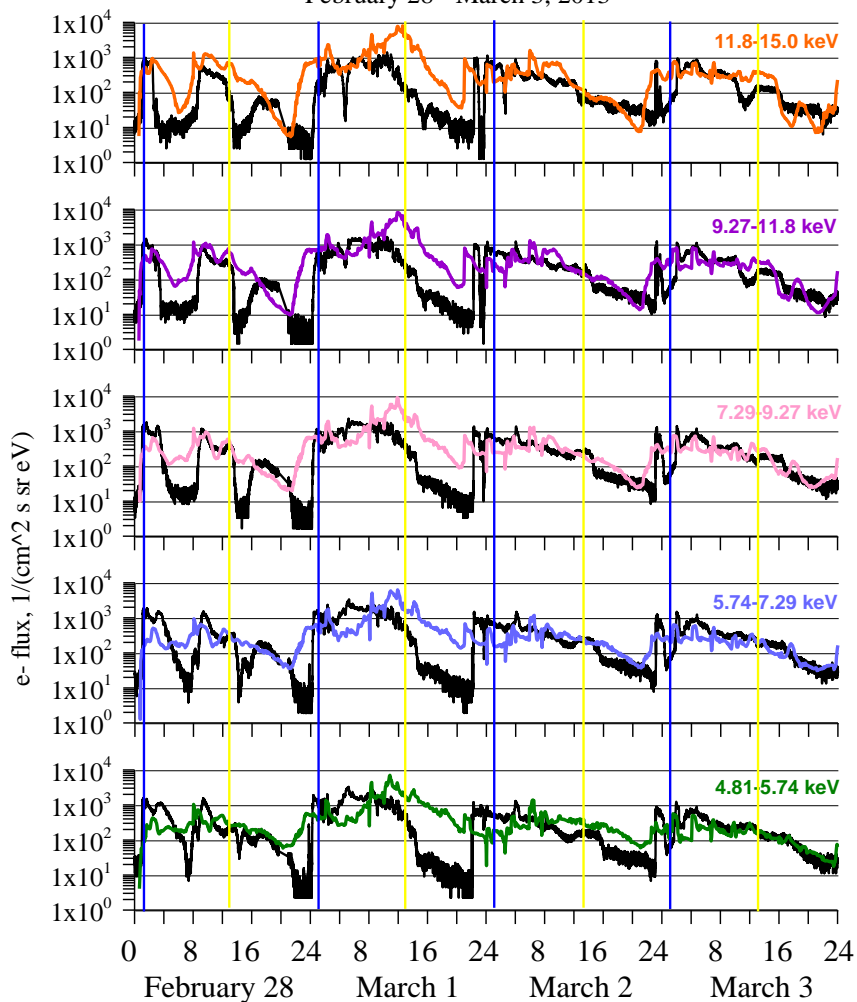
Electron fluxes observed by AMC 12 CEASE II ESA instrument for 5-15 keV energies and modeled
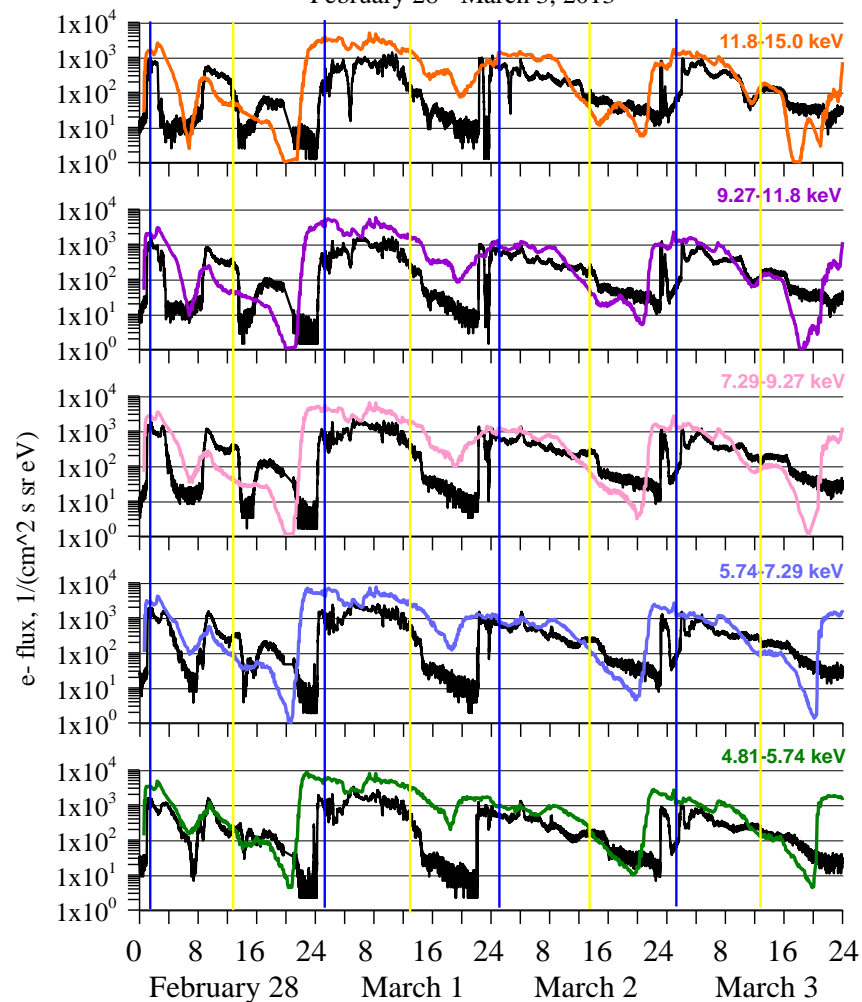
with **TM03** model and *Chen et al.* **[2005]** electron lifetimes for strong and *Shprits et al.* **[2007]** for weak diffusion

With **THEMIS** model and *Orlova and Shprits* **[2014] and** *Orlova et al.* **[2014]** electron lifetimes

Near-real time IMPTAM model for low energy electrons (*Ganushkina et al., 2013, 2014, 2015*)

What do we present?

IMPTAM (Inner Magnetosphere Particle Transport and Acceleration model): nowcast model for low energy (< 200 keV) electrons in the near-Earth geospace, operating online at **http://fp7-spacecast.eu** and **imptam.fmi.fi**

Why this model is important?

Low energy electron fluxes are very important to specify when hazardous satellite **surface charging** phenomena are considered.

They constitute the low energy part of the seed population for the high energy MeV particles in the **radiation belts**

What does the model provide?

The presented model provides the low energy electron flux at all locations and at all satellite orbits, when necessary, in the near-Earth space.

What are the drivers of the model?

The model is driven by the real time solar wind and Interplanetary Magnetic Field parameters with 1 hour time shift for propagation to the Earth's magnetopause, and by the real time geomagnetic activity index Dst.

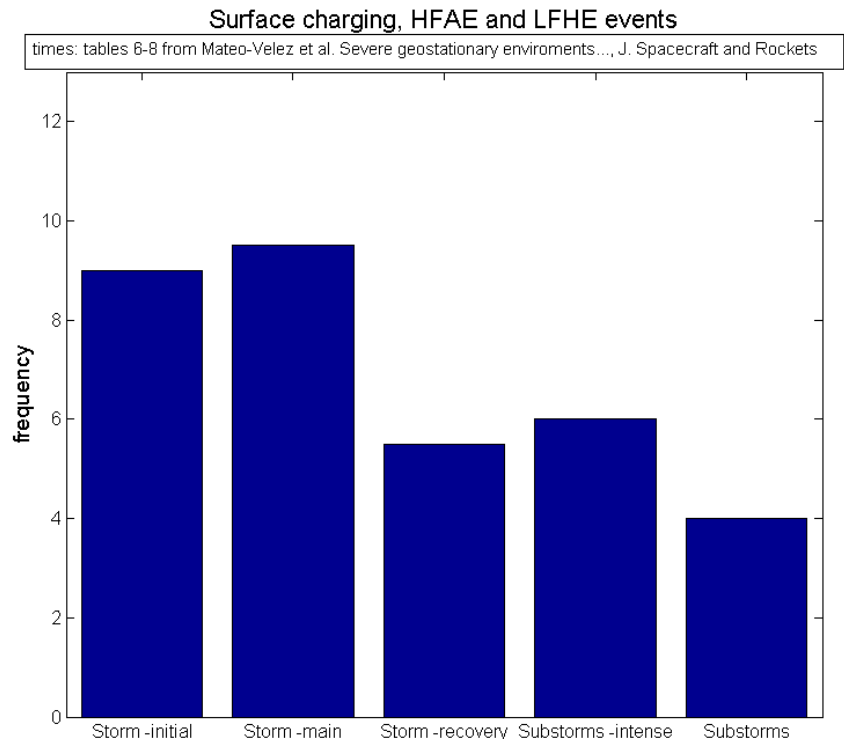# It is challenging to nowcast and forecast low energy electrons

Surface charging events vs. geomagnetic conditions

It is NOT necessary to have even a moderate storm for significant surface charging event to happen

The keV electron flux is largely determined by convective and substorm-associated electric fields and varies significantly with geomagnetic activity – variations on time scales of minutes!
No averaging over an hour/day/orbit!

Correct models for electromagnetic fields, boundary conditions, losses are extremely hard to develop

Surface charging, HFAE and LFHE events

times: tables 6-8 from Mateo-Velez et al. Severe geostationary enviroments..., J. Spacecraft and Rockets

Matéo Vélez et al., Severe geostationary environments: from flight data to numerical estimation of spacecraft surface charging, *Journal of Spacecraft and Rockets, submitted, 2015*
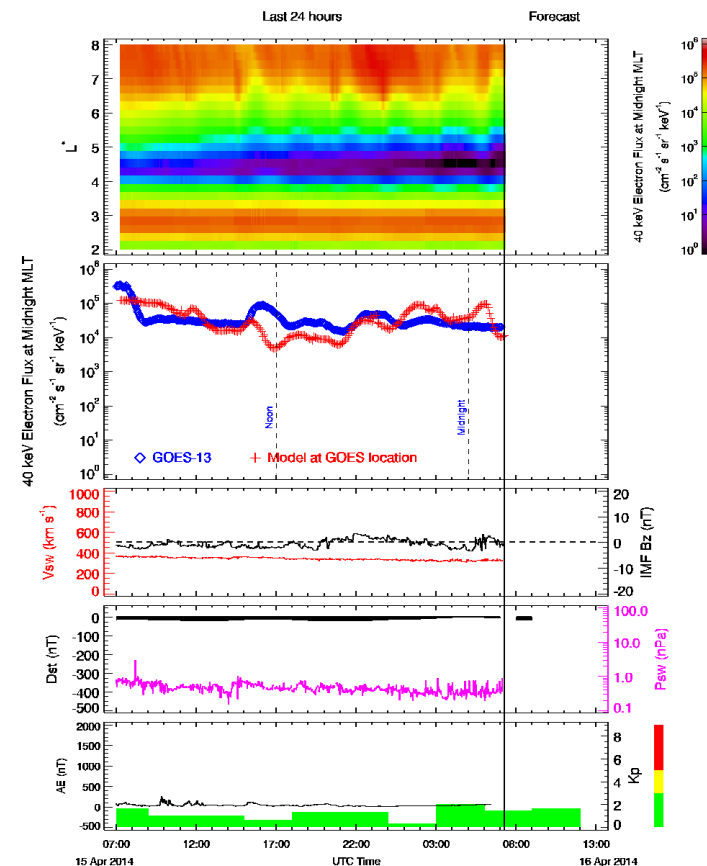
http://fp7-spacecast.eu

Low Energy Electrons Nowcast

40 keV

75 keV

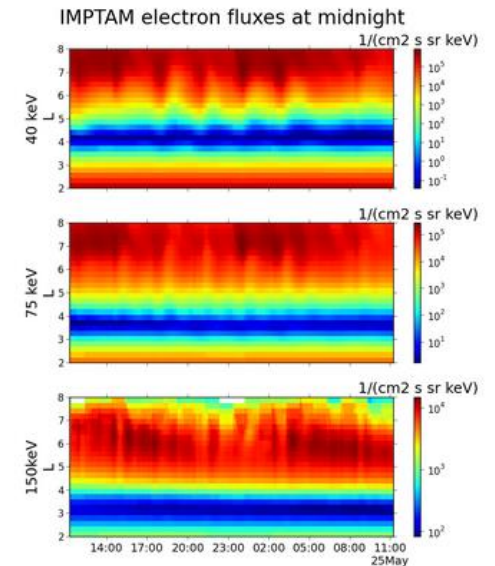150 keV

Compared to GOES 13 MAGED electron data

imptam.fmi.fi
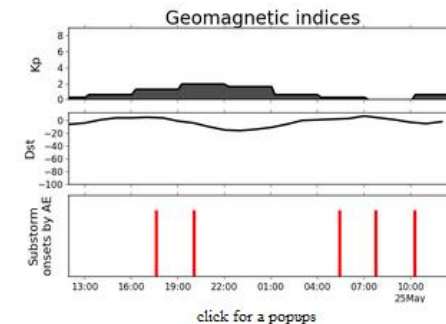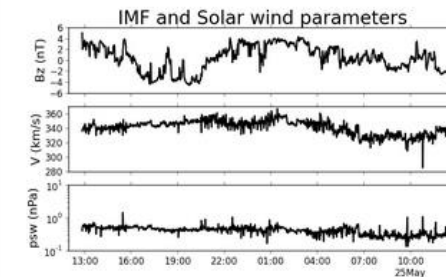
Low Energy Electrons Nowcast
40 keV
75 keV
150 keV
Compared to GOES 13 MAGED
electron data

Main points (1)

1. Different combinations of the magnetic and electric field models and boundary conditions result in very different modeled ring current, and, therefore, the physical conclusions based on simulation results can differ significantly.

Can we be sure that something is better?

2. A time-dependent model boundary outside of 6.6 RE gives a possibility to take into account the particles in the transition region (between dipole and stretched field lines) forming a partial ring current and near-Earth tail current in that region.

RC inside 6.6 Re has no sense?

Boundary conditions in the plasma sheet.

3. Calculating the model Dst* by Biot-Savart's law instead of the widely used Dessler-Parker-Sckopke (DPS) relation gives larger and more realistic values, since the contribution of the near-Earth tail current can be present.

Tail current is important and has to be considered

Main points (2)

4. Including self-consistent magnetic field when modeling with realistic background magnetic field model but with model ring and tail currents removed

Can we just use realistic magnetic field models and not include self-consistency?

5. **Substorm-associated fields must be taken into account when modeling ring current**.

6. Ion composition from Polar CAMMICE/MICS

Initial phase: almost similar contributions from ion species (He+,++, O+,++), no dependence on Dst

Main phase: larger contribution from He+ and He++ (1 order of magnitude increase), O+,++ contribution increase to 2 orders of magnitude with Dst decrease

Recovery phase order of magnitude difference between He+,++ and O+,++ contributions, decrease with Dst increase

No clear indication when O+ can be really dominant

Main points (3)

7. Real-time geostationary GOES 13 MAGED data on electron fluxes for three energies of 40, 75, and 150 keV are used for comparison and validation of IMPTAM in statistical sense by dependencies on IMF and SW parameters and activity indices for time period between September 2013 and March 2015.

Ongoing IMPTAM-online improvement: introducing empirical model for boundary conditions in the plasma sheet based on THEMIS data, launching electromagnetic pulses on substorm onsets determined by AE index in real time.

Good performance model for keV electron fluxes for surface charging effects!